

DRIVEARENA: A CLOSED-LOOP GENERATIVE SIMULATION PLATFORM FOR AUTONOMOUS DRIVING

Anonymous authors

Paper under double-blind review

ABSTRACT

This paper introduces DRIVEARENA, the first high-fidelity closed-loop simulation system designed for driving agents navigating real-world scenarios. DRIVEARENA comprises two core components: Traffic Manager, a traffic simulator capable of generating realistic traffic flow on any global street map, and World Dreamer, a high-fidelity conditional generative model with infinite auto-regression. DRIVEARENA supports closed-loop simulation using road networks from cities worldwide, enabling the generation of diverse traffic scenarios with varying styles. This powerful synergy empowers any driving agent capable of processing real-world images to navigate in DRIVEARENA’s simulated environment. Furthermore, DRIVEARENA features a flexible, modular architecture, allowing for multiple implementations of its core components and driving agents. Serving as a highly realistic *arena* for these *players*, our work provides a valuable platform for developing and evaluating driving agents across diverse and challenging scenarios. DRIVEARENA takes a significant leap forward in leveraging generative models for driving simulation platforms, opening new avenues for closed-loop evaluation of autonomous driving systems.

Codes of DRIVEARENA are attached to the supplementary material.

Project Page: <https://blindpaper.github.io/DriveArena/>

1 INTRODUCTION

Autonomous driving (AD) algorithms have advanced rapidly in recent decades (Ayoub et al., 2019; Chen et al., 2023; Xing et al., 2021; Ma et al., 2023; Yang et al., 2021; Mei et al., 2023c;b;a; 2024b), progressing from modular pipelines (Yin et al., 2021; Guo et al., 2023b; Li et al., 2023d; 2022b) to end-to-end models (Hu et al., 2023b; Ye et al., 2023; Jiang et al., 2023) and knowledge-driven methods (Li et al., 2023c; Wen et al., 2023b; Fu et al., 2024b). Despite demonstrating outstanding performance across various benchmarks, significant challenges persist in evaluating these algorithms on replayed open-loop datasets, obscuring their real-world efficacy. Public datasets (Caesar et al., 2020; 2021; Sun et al., 2020), while offering realistic driving data with authentic sensor inputs and traffic behavior, are inherently biased towards simple straight-ahead scenarios. In such cases, an agent can achieve seemingly good performance by merely maintaining its current state, complicating the assessment of actual driving capabilities in complex situations. Furthermore, the agent’s current decision does not affect execution or subsequent decisions in the open-loop evaluation, which prevents it from reflecting cumulative errors in real-world driving scenarios. Additionally, the static nature of recorded datasets, where other vehicles cannot react to the ego vehicle’s behavior, further hinders the evaluation of AD algorithms in dynamic, real-world conditions.

As illustrated in Figure 1, we analyze existing AD methods and platforms, revealing that most of them are inadequate for a high-fidelity closed-loop simulation. Ideally, as an aspect of embodied intelligence, agents should be evaluated in a closed-loop environment, where other agents react to the actions of the ego vehicle, and the ego vehicle receives changed sensor input accordingly. However, existing simulation environments either cannot simulate sensor inputs (Wen et al., 2023c; Krajzewicz et al., 2012; Gulino et al., 2024) or have a significant domain gap with the real world (Dosovitskiy et al., 2017; Li et al., 2022a), making it difficult to seamlessly integrate algorithms into the real world, thus posing a huge challenge for closed-loop evaluation. We believe that the simulator should not only closely reflect the visual and physical aspects of the real world, but also promote the continuous

learning and evolution of the model within an exploratory closed-loop system for adapting to diverse complex driving scenarios. To achieve this goal, it is imperative to establish a high-fidelity simulator that complies with physical laws and supports interactive functionalities.

Therefore, we present DRIVEARENA, a pioneering closed-loop simulator based on conditional generative models for training and testing driving agents. Specifically, DRIVEARENA offers a flexible platform that can be integrated with any camera-input driving agent. It adopts a modular design and naturally supports iterative upgrades of each module. DRIVEARENA consists of a Traffic Manager that manages traffic flow and a World Dreamer based on autoregressive generation. Traffic Manager can generate realistic interactive traffic flow on any road network worldwide, while World Dreamer is a high-fidelity conditional generative model with infinite autoregression. The driving agent should make corresponding driving actions based on the images generated by World Dreamer, and feed them back to Traffic Manager to update the status of vehicles in the environment. The new scene layout will be returned to World Dreamer for a new round of simulation. This iterative process realizes the dynamic interaction between the driving agent and the simulation environment. The specific contributions are as follows:

- **High-fidelity Closed-loop Simulation:** We propose the first high-fidelity closed-loop simulation platform for autonomous driving, DRIVEARENA, which can provide realistic surround images and integrate seamlessly with existing vision-based driving agents. DRIVEARENA closely reflects the visual and physical properties of the real world, enabling agents to continuously learn and evolve in a closed-loop manner and adapt to various complex driving scenarios.
- **Controllability and Scalability:** Our Traffic Manager can dynamically control the movement of all vehicles in the scenarios and feed the road and vehicle layouts into World Dreamer, which utilizes a conditional diffusion framework to generate realistic images in a stable and controllable manner. Additionally, DRIVEARENA supports simulation using road networks from any city worldwide, enabling the creation of diverse driving scenario images with varying styles.
- **Modularized Design:** The Driving Agent, Traffic Manager and World Dreamer communicate via network interfaces, enabling a highly flexible and modular framework. This architecture allows each component to be replaced with different methods without requiring specific implementations. Functioning as an *arena* for these *players*, DRIVEARENA facilitates comprehensive testing and improvement of both vision-based driving agents and driving scene generative models.

2 DRIVEARENA FRAMEWORK

As illustrated in Figure 2, the framework of our proposed DRIVEARENA comprises two key components: a Traffic Manager functioning as the backend physical engine and a World Dreamer serving as the real-world image renderer. Notably, DRIVEARENA does not rely on pre-built digital assets or reconstructed 3D road models. Instead, the Traffic Manager adapts to road networks of any city in OpenStreetMap (OSM) format (Haklay & Weber, 2008), which can be directly downloaded from the Internet. This flexibility enables closed-loop traffic simulations on diverse urban layouts.

The Traffic Manager receives ego trajectories output by the autonomous driving agent and manages the movement of all background vehicles. Unlike world model approaches (Gao et al., 2023; Hu

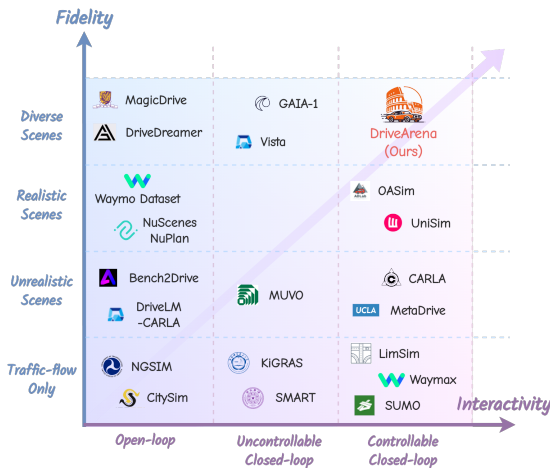


Figure 1: Comparison of DRIVEARENA with existing autonomous driving methods and platforms along the dimensions of Interactivity and Fidelity. *Interactivity* indicates the platform’s control over vehicles, *Fidelity* reflects the realism of driving scenarios. DRIVEARENA uniquely occupies the top-right, being the first simulation platform to generate diverse traffic scenarios and surround-view images with closed-loop controllability for all vehicles. For detailed descriptions of these methods and related works, please refer to Table 4 and Appendix A.1.

108
109
110
111
112
113
114
115
116
117
118
119
120
121
122
123
124
125
126
127
128
129
130
131
132
133
134
135
136
137
138
139
140
141
142
143
144
145
146
147
148
149
150
151
152
153
154
155
156
157
158
159
160
161

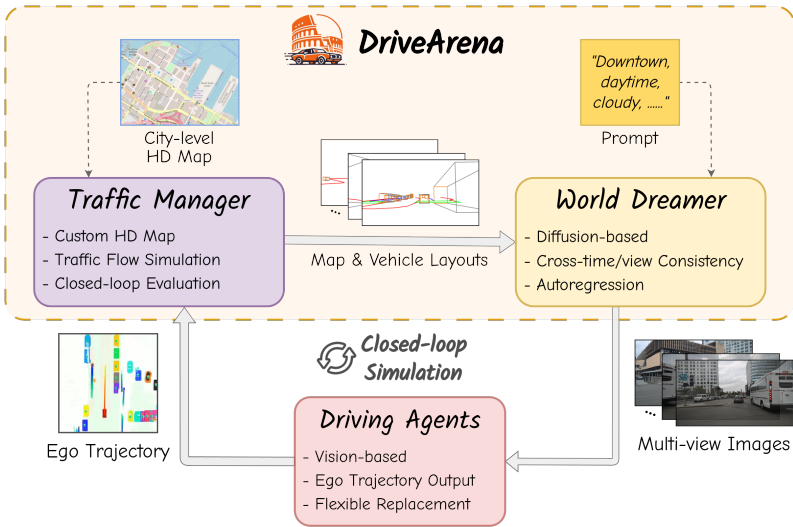


Figure 2: Overview of the DRIVEARENA framework. The system consists of two main components: (1) The Traffic Manager, which processes Internet-downloaded HD maps to create diverse urban layouts, manages vehicle movements including background traffic, and handles collision detection. (2) The World Dreamer, an auto-regressive generative model that generates photo-realistic, multi-view camera images corresponding to the simulation state, with controllable parameters following given prompts. The framework operates in a closed loop: generated images are fed to the AD agent, which outputs the planned ego trajectory. The trajectory is then fed back into the Traffic Manager for the next simulation step.

et al., 2023a) that rely on diffusion models for both image generation and vehicle movement prediction, our Traffic Manager utilizes explicit traffic flow generation algorithms (Wen et al., 2023a). This approach enables the generation of a wider range of uncommon and potentially unsafe traffic scenarios, while also facilitating real-time collision detection between vehicles.

World Dreamer generates realistic camera images that precisely correspond to the Traffic Manager’s output. It also allows for user-defined prompts to control various elements of the generated images, such as street view style, time of day, and weather conditions, enhancing the diversity of the generated scenes. Specifically, it employs a diffusion-based model that utilizes the current map and vehicle layouts as control conditions to produce surround-view images. These images serve as input for end-to-end driving agents. Given DRIVEARENA’s closed-loop architecture, the diffusion model is required to maintain both cross-view and temporal consistency in the generated images.

The generated multi-view images of the current frame are fed into the end-to-end autonomous driving agents, which can output the ego vehicle’s movement. The planned ego trajectory is subsequently sent to DRIVEARENA for the next simulation step. The simulation concludes when the ego vehicle either successfully completes the entire route, crashes, or deviates from the road. Upon completion, DRIVEARENA performs a comprehensive evaluation process to assess the agent’s capabilities.

It is noteworthy that DRIVEARENA employs a distributed modular design. The Traffic Manager, World Dreamer, and AD agent communicate via network using standardized interfaces. Consequently, DRIVEARENA does not mandate specific implementations of individual modules and the AD agent. Our framework aims to function as an “arena” for these “players”, facilitating comprehensive testing and improvement of both end-to-end autonomous driving algorithms and realistic driving scene generative models.

3 METHODOLOGY

Following the DRIVEARENA framework outlined above, we have implemented a preliminary version of DRIVEARENA. In this section, we elaborate on the implementation of each module: Traffic Manager, World Dreamer, and AD agent, while describing necessary details that were not previously

162 mentioned. At the end of this section, we present both the open-loop and closed-loop evaluation
163 metrics for AD agents in DRIVEARENA.
164

165 3.1 TRAFFIC MANAGER 166

167 Most existing realistic driving simulators (Yan et al., 2024; Yang et al., 2023b; Wu et al., 2023) rely
168 on limited layouts from public datasets, lacking diversity for dynamic environments. To address
169 these challenges, we utilize LimSim (Wen et al., 2023c; Fu et al., 2024a) as the underlying Traffic
170 Manager to simulate dynamic traffic scenarios and generate road and vehicle layouts for subsequent
171 environment generation. LimSim also provides a user-friendly front-end GUI, which directly dis-
172 plays the BEV map and results from World Dreamer and the driving agent.

173 Our Traffic Manager enables interactive simulations of multiple vehicles in traffic flow, including
174 comprehensive vehicle planning and control. We adopt a hierarchical multi-vehicle decision-making
175 and planning framework, which jointly makes decisions for all vehicles within the flow and re-
176 acts promptly to the dynamic environment through a high-frequency planning module (Wen et al.,
177 2023a). The framework also incorporates a cooperation factor and trajectory weight set, introducing
178 diversity to autonomous vehicles in traffic at both social and individual levels.

179 Furthermore, our dynamic simulator supports various custom HD maps of any city from Open-
180 StreetMap, facilitating the construction of diverse road graphs for convenient simulation. The Traf-
181 fic Manager controls the movement of all background vehicles. For the ego vehicle, we provide
182 two distinct simulation modes: open-loop and closed-loop. In closed-loop mode, the driving agent
183 performs planning for the ego vehicle, and Traffic Manager uses the agent-outputted trajectory to
184 control the ego vehicle accordingly. In open-loop mode, the trajectory generated by the driving
185 agent is not actually used to control the ego vehicle; instead, Traffic Manager maintains control in a
186 closed-loop manner. The details of these two modes are further elaborated in Section 3.4.
187

188 3.2 WORLD DREAMER 189

190 Unlike recent autonomous driving generation methods (Yan et al., 2024; Yang et al., 2023b; Wu
191 et al., 2023) that use Neural Radiance Fields (NeRF) and 3D Gaussian Splatting (3D GS) for envi-
192 ronment reconstruction from logged video, we design a diffusion-based World Dreamer. It utilizes
193 control conditions of the map and object layouts from the Traffic Manager to generate geometri-
194 cally and contextually accurate driving scenarios. Our framework shares several advantages: (1)
195 Better controllability. The generated scenes can be controlled by scene layouts from Traffic Man-
196 ager, textual prompts, and reference images to capture different weather conditions, lighting, and
197 scene styles. (2) Better scalability. Our framework can be adapted to various road structures without
198 the need to model the scene in advance. In theory, we support the generation for any city using
199 OpenStreetMap layouts. [However, we acknowledge that compared to NeRF and 3D GS methods, our WorldDreamer currently exhibits limitations in maintaining strict geometric and semantic consistency due to the absence of explicit 3D model constraints.](#)
200

201 We illustrate our diffusion-based World Dreamer in Figure 3. Built upon the stable diffusion pipeline
202 (Blattmann et al., 2023), World Dreamer utilizes an effective condition encoding module that accepts
203 a variety of conditional inputs including map and object layouts, text descriptions, camera parame-
204 ters, ego poses, and reference images to generate realistic surround-view images. Considering the
205 importance of ensuring synthesis scene consistency across different views and time spans for driving
206 agents, we integrate a cross-view attention module, inspired by (Gao et al., 2023), to maintain coher-
207 ence across different views. Additionally, we adopt an image auto-regressive generation paradigm to
208 enforce temporal consistency. This approach enables World Dreamer to not only maximally main-
209 tain the temporal consistency of the generated videos, but also generate videos of arbitrary length in
210 an infinite stream, which provides great support for autonomous driving simulation.

211 **Condition encoding.** Previous work (Gao et al., 2023) applied the BEV layout as a conditional
212 input to control the output of the diffusion model, increasing the difficulty of the network in learn-
213 ing to generate geometrically and contextually accurate driving scenes. In this work, we intro-
214 duce more guidance information that helps the model generate high-fidelity surround images. In
215 addition to encoding camera poses for each view, text descriptions, 3D object bounding boxes,
and BEV maps using a condition encoder similar to (Gao et al., 2023), we also explicitly project

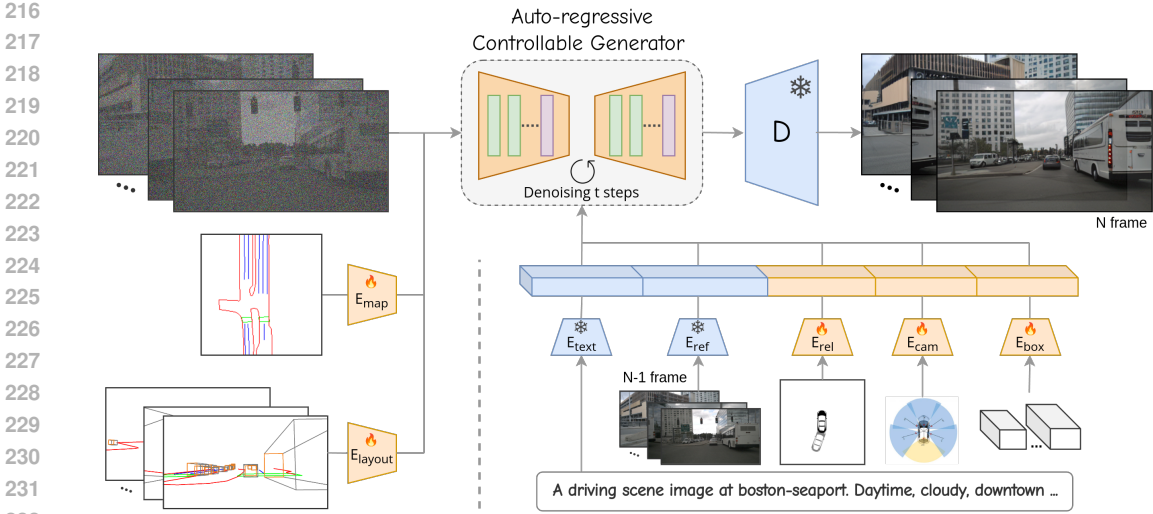


Figure 3: The figure illustrates the denoising process employed by World Dreamer. Beginning with randomly sampled noise, the autoregressive model utilizes various conditions—such as multi-view layout, BEV map, text prompt, reference image, relative pose, camera parameters, and 3D bounding boxes—to enhance the denoising procedure. The encoders depicted in the figure are distinct, with the color indicating whether each one utilizes a pre-trained network or is frozen. Additionally, we incorporate ControlNet to introduce conditional control into the diffusion model.

the map and object layouts onto each camera view to generate layout canvases for more accurate lane and object generation guidance. Specifically, the text embedding e_{text} is obtained by encoding the text descriptions with the CLIP text encoder (Radford et al., 2021). The parameters $\mathbf{P} = \{\mathbf{K} \in \mathbb{R}^{3 \times 3}, \mathbf{R} \in \mathbb{R}^{3 \times 3}, \mathbf{T} \in \mathbb{R}^{3 \times 1}\}$ of each camera and the 8 vertices of the 3D bounding boxes are encoded to e_{cam} and e_{box} by Fourier embedding (Mildenhall et al., 2021), where \mathbf{K} , \mathbf{R} , \mathbf{T} represent camera intrinsic, rotations and translations respectively. The 2D BEV map grid uses the same encoding method as in (Gao et al., 2023) to obtain the embedding e_{map} . Then, each category of the HD maps and the 3D boxes is projected onto the image plane respectively to obtain the layout canvas. The final feature e_{layout} can be obtained by encoding the layout canvas by the conditional encoding network (Zhang et al., 2023).

Moreover, we introduce a reference condition to provide appearance and temporal consistency guidance. During training, we randomly extract a frame from the past n frames as a reference frame and use the pre-trained CLIP model (Radford et al., 2021) to extract reference features e_{ref} from the multi-view images. These features imply semantic context and are integrated into the conditional encoder through a cross-attention module. To enable the diffusion model to grasp how the ego-car’s motion influences background changes, we encode the ego-pose relative to the reference frame within the conditional encoder. The relative pose embedding e_{rel} is encoded by Fourier embedding. By incorporating the above control conditions, we can effectively control the generation of images.

Auto-regressive generation. To facilitate online inference and streaming video generation while maintaining temporal coherence, we have developed an auto-regressive generation pipeline. Specifically, during the inference phase, the previously generated images and the corresponding relative ego pose are used as reference conditions. This approach guides the diffusion model to generate current surround images with enhanced consistency, ensuring a smoother transition and coherence with the previously generated frames.

This paper presents a simple implementation of World Dreamer. We also verify that extending to a multi-frame auto-regressive version (using multiple past frames as reference and outputting multi-frame images) and adding additional temporal modules can enhance temporal consistency.

3.3 DRIVING AGENT

Recent works (Li et al., 2024; Zhai et al., 2023) have demonstrated the challenges in justifying the planning behavior of driving agents through open-loop evaluation on public datasets (Caesar et al.,

270 2020), primarily due to the simplistic nature of driving scenarios presented. While some studies
 271 (Wang et al., 2023a) have conducted closed-loop evaluations using simulators like CARLA (Doso-
 272 vitskiy et al., 2017), discrepancies such as appearance and scene diversity persist between these
 273 simulations and the dynamic real world. To bridge this gap, our DRIVEARENA provides a realistic
 274 simulation platform with the corresponding interfaces for camera-based driving agents (Jiang et al.,
 275 2023; Hu et al., 2023b; 2022) to perform more comprehensive evaluations, including both open-loop
 276 and closed-loop testing. Moreover, by changing the input conditions, such as the road and vehicle
 277 layouts, DRIVEARENA could generate corner cases and facilitate these driving agents’ evaluation
 278 on out-of-distribution scenarios. Without loss of generality, we select two representative end-to-end
 279 driving agents, namely UniAD (Hu et al., 2023b) and VAD Jiang et al. (2023), for open-loop and
 280 closed-loop testing in our DRIVEARENA. They utilize surround images to predict motion trajec-
 281 tories for the ego vehicle and other agent vehicles, which can be seamlessly integrated with our
 282 Traffic Manager for evaluation. Furthermore, the perceptual outputs, such as 3D detection and map
 283 segmentation, contribute to enhancing the validation of realism in our environment generation.

284 3.4 EGO CONTROL MODES AND EVALUATION METRICS

286 DRIVEARENA inherently supports “closed-loop” simulation mode of driving agents. That is, the
 287 system adopts the trajectory output by the agent at each timestep, updates the ego vehicle’s state
 288 based on this trajectory, and simulates the actions of background vehicles. Subsequently, it gener-
 289 ates multi-view images for the next timestep, thus maintaining a continuous feedback closed-loop.
 290 Additionally, recognizing that some AD agents may be unable to perform long-term closed-loop
 291 simulation during the development process, DRIVEARENA also supports the “open-loop” simula-
 292 tion mode. In this mode, the Traffic Manager will take over the control of the ego vehicle, while the
 293 trajectory output by the AD agent is recorded for subsequent evaluation.

294 In both open-loop and closed-loop modes, it is crucial to comprehensively evaluate AD agent perfor-
 295 mance from a results-oriented perspective. Drawing inspiration from NAVSIM (Dauner et al., 2024)
 296 and the CARLA Autonomous Driving Leaderboard (CARLA Team et al., 2023), DRIVEARENA
 297 adopts two evaluation metrics: PDM Score (PDMS) and Arena Driving Score (ADS).

298 PDMS, initially proposed by NAVSIM (Dauner et al., 2024), evaluates the trajectory output at each
 299 timestep. We adhere to the original definition of PDMS, which aggregates the following sub-scores:

$$301 \text{ PDMS}_t = \underbrace{\left(\prod_{m \in \{NC, DAC\}} \text{score}_m \right)}_{\text{penalties}} \times \underbrace{\left(\frac{\sum_{w \in \{EP, TTC, C\}} \text{weight}_w \times \text{score}_w}{\sum_{w \in \{EP, TTC, C\}} \text{weight}_w} \right)}_{\text{weighted average}}. \quad (1)$$

306 where the penalties include the drive with no collisions (NC) with road users and drivable area
 307 compliance (DAC), as well as the weighted average, including ego progress (EP), time-to-collision
 308 (TTC), and comfort (C). We implement minor modifications tailored to DRIVEARENA: in score_{NC},
 309 we do not differentiate “at-fault” collisions, and for score_{EP}, we utilize the Traffic Manager’s Ego
 310 path planner as the reference trajectory instead of the Predictive Driver Model. At the end of the
 311 simulation, the final PDM Score is averaged across all simulation frames.

$$312 \text{ PDMS} = \frac{\sum_{t=0}^T \text{PDMS}_t}{T} \in [0, 1] \quad (2)$$

316 For open-loop simulations, PDMS serves directly as the evaluation metric for AD agents. However,
 317 for agents operating under the “closed-loop” simulation mode, we employ a more comprehensive
 318 metric called Arena Driving Score (ADS), which combines the PDMS with route completion:

$$319 \text{ ADS} = R_c \times \text{PDMS} \quad (3)$$

321 where $R_c \in [0, 1]$ represents route completion, defined as the percentage of the route distance com-
 322 pleted by an agent. Given that “closed-loop” simulations terminate upon agent collision with other
 323 road users or deviation from the road, ADS provides a suitable metric for differentiating agents’
 driving safety and consistency.

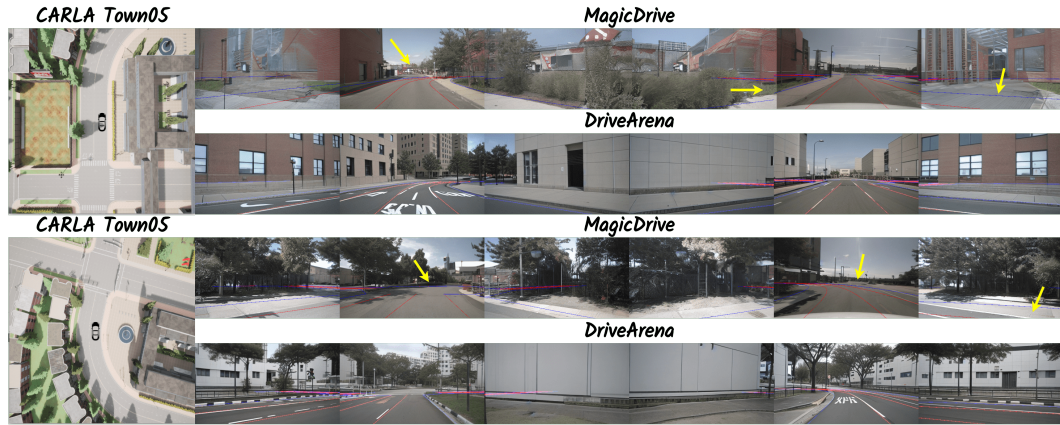


Figure 4: Comparison between MagicDrive and DRIVEARENA. Both are used to generate realistic images on the same Carla Town05 Map, with corresponding ground truth lane lines projected onto the images for demonstration. For such large curvatures and wide roads in CARLA, which are atypical scenarios in the nuScenes dataset, MagicDrive struggles to generate images that accurately fit the network. It incorrectly generates pavements and fails to match the road curvature (indicated by yellow arrows). In contrast, DRIVEARENA successfully generates images that accurately represent the road structure.

4 EXPERIMENTS

4.1 EXPERIMENTAL SETUPS

For World Dreamer, we use the nuScenes (Caesar et al., 2020) dataset for training. The nuScenes dataset contains data collected from four different cities, covering various lighting and weather conditions, allowing DRIVEARENA to conditionally imitate different appearances. The model is initialized using the pre-trained Stable Diffusion v1.5 (Rombach et al., 2022), and various control conditions are integrated into UNet with a randomly initialized ControlNet (Zhang et al., 2023) to control the denoising process. The experiment is conducted on 8 NVIDIA A100 (80GB) GPUs with a batch size of 4×8 and 200K training iterations.

Traffic Manager operates at 10Hz, while the control frequency is set to 2Hz to accommodate the AD agents. We implement two simulation modes: open-loop and closed-loop. In closed-loop mode, the simulation terminates if it crashes with other vehicles or leaves the road. Currently, DRIVEARENA supports four different maps: `singapore-onenorth`, `boston-seaport`, `boston-thomaspark`, and `carla-town05`. In fact, Traffic Manager can download road network data for any area directly from OpenStreetMap¹ and perform simulations, enabling DRIVEARENA to simulate the road network of almost any city worldwide. Please refer to Appendix A.2 for more implementation details.

4.2 WORLD DREAMER PERFORMANCE ASSESSMENT

Fidelity. In this section, we assess the sim-to-real gap between our generated images and the original nuScenes images. We generate videos based on the original layout provided by the nuScenes validation set with 2Hz. For comparative analysis, we set MagicDrive as the baseline method perform the same inference using its official code and checkpoints. Subsequently, UniAD is performed as an evaluator on these images to compute various metrics, including 3d object detection, BEV map segmentation, and planning. The results are summarized in Table 1. It shows that all our indicators are higher than the baseline method, and a few indicators even surpass the performance on the original nuScenes. Furthermore, it demonstrates our model’s superior capability to accurately respond to control signals and strictly adhere to input conditions. These findings establish a solid foundation for using our generator as a reliable simulator.

¹<https://www.openstreetmap.org/>

Table 1: Comparison of generation fidelity. The data synthesis conditions are from the nuScenes validation set. All results are computed by using the official implementation and checkpoints of UniAD. **Bold** represents the best results, underline represents the second best results.

Data Source	3DOD		BEV Segmentation mIoU (%)				L2 (m) ↓				Col. Rate (%) ↓			
	mAP ↑	NDS ↑	Lanes ↑	Drivable ↑	Divider ↑	Crossing ↑	1.0s	2.0s	3.0s	Avg.	1.0s	2.0s	3.0s	Avg.
ori nuScenes	37.98	49.85	31.31	69.14	25.93	14.36	0.51	0.98	1.65	1.05	<u>0.10</u>	0.15	<u>0.61</u>	<u>0.29</u>
MagicDrive	12.92	28.36	21.95	51.46	17.10	5.25	0.57	1.14	1.95	1.22	<u>0.10</u>	0.25	0.70	0.35
DRIVEARENA	<u>16.06</u>	<u>30.03</u>	<u>26.14</u>	<u>59.37</u>	<u>20.79</u>	<u>8.92</u>	<u>0.56</u>	<u>1.10</u>	<u>1.89</u>	<u>1.18</u>	0.02	<u>0.18</u>	0.53	0.24

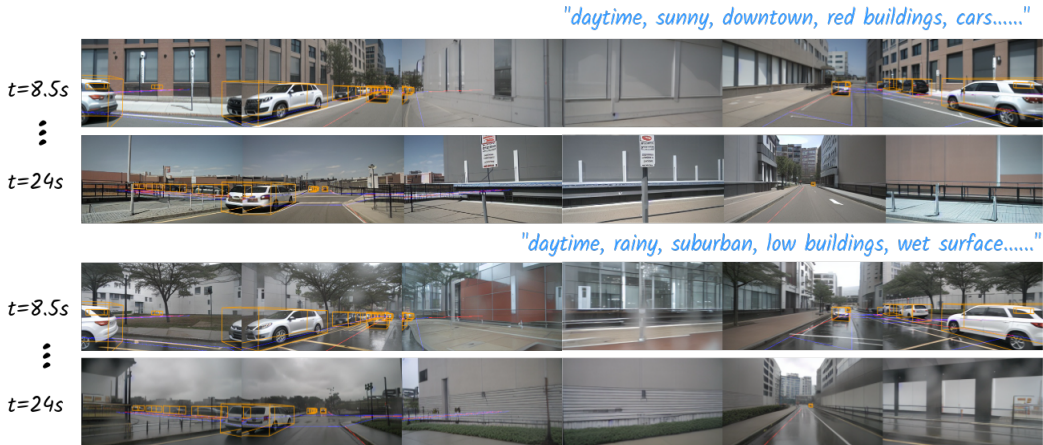


Figure 5: Demonstration of diverse prompts and reference images’ influence on identical scenes. The figure features two distinct image sequences generated by DRIVEARENA for the same 30-second simulation, each driven by different prompts and reference images. These sequences reveal clear contrasts in weather and lighting conditions while maintaining their individual styles consistently throughout the entire 30-second duration. For more driving scenes under different prompts and reference images, please refer to Figure 9 in Appendix A.3.

Controllability and Scalability. The Traffic Manager can accept any map downloaded from OpenStreetMap and seamlessly connect to the Carla road network. Combined with Dreamer’s excellent following capability, the entire framework demonstrates robust controllability and scalability. The specific results are shown in Figure 4. We used both MagicDrive and our World Dreamer to generate realistic images on the same Carla road network, with the corresponding lane lines projected onto the images. The road style in Carla differs significantly from that of nuScenes. It is rare to encounter roads with such large curvature and such wide roads in nuScenes. Consequently, the performance of MagicDrive, which is based on the nuScenes BEV map, is slightly inferior in these conditions. As indicated by the yellow arrow, MagicDrive struggles to generate curved roads and fit wide roads accurately. DRIVEARENA, however, can produce reasonable pictures that follow the road structure.

Figure 5 presents images generated using different text prompts and reference images on the same road network. Each set of images portrays the surrounding scenery at intervals of 8.5 seconds and 24 seconds respectively, with the layout projected on the image. The images clearly illustrate that the road structure and vehicles strictly adhere to the given control conditions while maintaining excellent consistency in the surrounding view. More examples are presented and discussed in Appendix A.3.

Furthermore, the road and vehicle layouts adhere to novel out-of-distribution scenario generation methods. Consequently, ARENA can generate corner cases such as head-on collisions and rear-end collisions. For a detailed elaboration on this aspect, please refer to Appendix A.5.

4.3 OPEN-LOOP AND CLOSED-LOOP EXPERIMENTS

In this section, we adopt the prevailing end-to-end autonomous driving methods UniAD (Hu et al., 2023b) and VAD (Jiang et al., 2023) as the driving agents to test both the open-loop and closed-loop performance within the DRIVEARENA framework. We utilized the open-source code and pre-trained

Table 2: Performance of driving agents in DRIVEARENA’s open-loop mode. Evaluation across three scenarios: 1) original nuScenes images sequences; 2) World Dreamer-generated images with nuScenes ground truth trajectories; and 3) DRIVEARENA’s open-loop mode simulation sequences. Metrics include: no collisions (NC), drivable area compliance (DAC), ego progress (EP), time-to-collision (TTC), comfort (C), and PDM Score (PDMS).

Scenario	Driving Agent	NC \uparrow	DAC \uparrow	EP \uparrow	TTC \uparrow	C \uparrow	PDMS \uparrow
nuScenes (original)	VAD	0.915 \pm 0.17	0.937 \pm 0.10	0.762 \pm 0.18	0.848 \pm 0.23	1.000\pm0.00	0.740 \pm 0.18
	UniAD	0.993\pm0.03	0.995\pm0.01	0.914\pm0.05	0.947\pm0.14	0.848 \pm 0.21	0.910\pm0.09
nuScenes (generated)	VAD	0.915 \pm 0.16	0.942 \pm 0.10	0.754 \pm 0.18	0.855 \pm 0.23	1.000\pm0.00	0.744 \pm 0.18
	UniAD	0.993\pm0.02	0.991\pm0.02	0.909\pm0.05	0.951\pm0.14	0.821 \pm 0.21	0.902\pm0.09
DRIVEARENA	VAD	0.807\pm0.11	0.950\pm0.05	0.795\pm0.13	0.800\pm0.12	0.913\pm0.09	0.683\pm0.12
	UniAD	0.792 \pm 0.11	0.942 \pm 0.04	0.738 \pm 0.11	0.771 \pm 0.12	0.749 \pm 0.16	0.636 \pm 0.08
nuScenes GT	Human	1.000 \pm 0.00	1.000 \pm 0.00	1.000 \pm 0.00	0.979 \pm 0.12	0.752 \pm 0.17	0.950 \pm 0.06

weights from the two driving agents without additional training. UniAD and VAD operate at 2Hz, outputting a trajectory of 6 path points over the next 3 seconds. Traffic Manager further interpolates this to a 10Hz trajectory.

Open-loop Evaluation. We first assess the performance of driving agents in DRIVEARENA’s open-loop mode. The agents are evaluated on three scenarios: 1) the original nuScenes image sequences; 2) World-Dreamer-generated nuScenes image sequences, where the vehicles’ trajectory remains identical to nuScenes ground truth, but surround images are replaced with World-Dreamer-generated ones; and 3) DRIVEARENA’s own simulation sequences (i.e., DRIVEARENA’s open-loop mode). Our evaluation metrics consist of the PDM Scores and its sub-scores, as detailed in Section 3.4. Additionally, we evaluate trajectories driven by human drivers in nuScenes as the human driver performance. Detailed results are presented in Table 2.

The results show that UniAD performs best on the original nuScenes sequence with a PDMS metric of 0.91, whereas the PDMS metric on the World Dreamer-generated sequence is a surprising 0.902, with a metric drop of less than 1%. We attribute this to both the high fidelity of our World Dreamer-generated images and UniAD’s dependence on ego states, as corroborated by (Li et al., 2024). Furthermore, VAD achieves better performance on the World Dreamer simulation sequences with a PDMS of 0.683, demonstrating its better open-loop ability on unseen roadmaps and scenarios. Figure 6 presents the open-loop performance of both driving agents in long simulation sequences. More examples of visualization of the open-loop evaluation can be found in Appendix A.4.

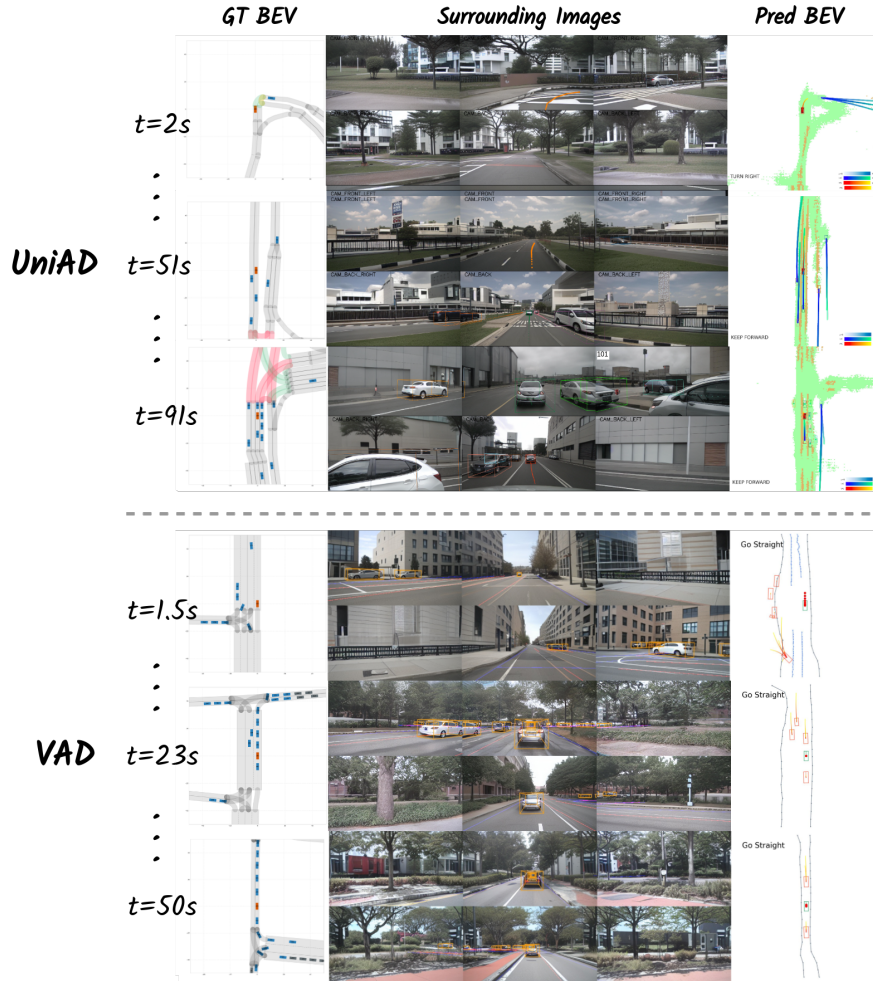
Closed-loop Evaluation. We further evaluate the performance of VAD and UniAD in DRIVEARENA’s closed-loop mode. In this mode, the trajectory outputted by the driving agents is directly used for ego vehicle control, and the evaluation metrics include PDM Score (PDMS), Route Completion (RC), and Arena Drive Score (ADS). Our closed-loop experiment was conducted on four pre-set paths, with two paths selected in Boston and two in Singapore. The simulation time to complete each route was approximately 120 seconds. Detailed results are presented in Table 3.

The results indicate that the PDMS of UniAD-generated trajectories in closed-loop mode (Avg.: 0.667) are comparable to those of the open-loop mode, while the PDMS of VAD-generated trajectories (Avg.: 0.534) has a significant metric drop of 0.149. The Route Completions (RC) of both driving agents are consistently low, with VAD completing just 4.59% and UniAD completing an average of 13.7% of the route. During the evaluation, both agents performed better on straightaways but largely failed to navigate the first turning intersection in the route. While VAD showed better metrics in open-loop mode, it failed to achieve better results when conducting closed-loop experiments. This highlights the inherent flaws of open-loop

Table 3: Evaluation of Driving Agents’ performance in DRIVEARENA’s closed-loop mode across four distinct routes. Performance metrics include: PDM Score (PDMS), Route Completion (RC), and Arena Driving Score (ADS).

Route	Driving Agent	PDMS \uparrow	RC \uparrow	ADS \uparrow
sing_route_1	VAD	0.5315	0.0467	0.0248
	UniAD	0.7615	0.1684	0.1282
sing_route_2	VAD	0.5147	0.0400	0.0206
	UniAD	0.7215	0.169	0.0875
bos_route_1	VAD	0.5830	0.0604	0.0352
	UniAD	0.4952	0.091	0.0450
bos_route_2	VAD	0.5054	0.0366	0.0185
	UniAD	0.6888	0.121	0.0835

486 evaluation in assessing the true capabilities of agents, which could potentially be mitigated by
 487 DRIVEARENA. See Appendix A.4 for the visualization of the failure cases in DRIVEARENA closed-
 488 loop mode.
 489



522 Figure 6: Case studies on open-loop performance of driving agents in DRIVEARENA. Two long-
 523 term open-loop simulation sequences are shown: the upper sequence depicts the performance of the
 524 uniad on the road network and style (left-hand drive) in Singapore, while the lower sequence shows
 525 the performance of VAD on the road network and style (right-hand drive) in Boston. Each subfig-
 526 ure shows, in order from left to right: ground truth BEVs from Traffic Manager; World Dreamer-
 527 generated images; and agent-predicted BEV images. For more open-loop case illustrations, please
 528 refer to Figure 12 and 13 in Appendix A.4.
 529

530 5 CONCLUSIONS

532 This paper introduces a novel closed-loop simulation platform named DRIVEARENA for vision-
 533 based driving agents. DRIVEARENA integrates a Traffic Manager that generates human-like traffic
 534 flow and a high-fidelity generative World Dreamer with infinite generation. This combination al-
 535 lows realistic interaction and continuous feedback between the driving agent and the simulation
 536 environment. The system provides a valuable platform for developing and testing autonomous
 537 driving agents in a variety of scenarios, marking a substantial leap in driving simulation technol-
 538 ogy. DRIVEARENA is designed with a modular architecture, allowing for easy replacement of each
 539 module. As the first high-fidelity closed-loop simulator, we still have a few limitations for future
 improvement, which are discussed in detail in Appendix A.6.

REFERENCES

- 540
541
542 Jackie Ayoub, Feng Zhou, Shan Bao, and X Jessie Yang. From manual driving to automated driving:
543 A review of 10 years of autou. In *Proceedings of the 11th international conference on automotive*
544 *user interfaces and interactive vehicular applications*, pp. 70–90, 2019.
- 545 Andreas Blattmann, Tim Dockhorn, Sumith Kulal, Daniel Mendelevitch, Maciej Kilian, Dominik
546 Lorenz, Yam Levi, Zion English, Vikram Voleti, Adam Letts, et al. Stable video diffusion: Scaling
547 latent video diffusion models to large datasets. *arXiv preprint arXiv:2311.15127*, 2023.
- 548 Daniel Bogdoll, Yitian Yang, and J Marius Zöllner. Muvo: A multimodal generative world model
549 for autonomous driving with geometric representations. *arXiv preprint arXiv:2311.11762*, 2023.
- 550
551 Holger Caesar, Varun Bankiti, Alex H Lang, Sourabh Vora, Venice Erin Liong, Qiang Xu, Anush
552 Krishnan, Yu Pan, Giancarlo Baldan, and Oscar Beijbom. nuscenes: A multimodal dataset for
553 autonomous driving. In *Proceedings of the IEEE/CVF conference on computer vision and pattern*
554 *recognition*, pp. 11621–11631, 2020.
- 555 Holger Caesar, Juraj Kabzan, Kok Seang Tan, Whye Kit Fong, Eric Wolff, Alex Lang, Luke Fletcher,
556 Oscar Beijbom, and Sammy Omari. nuplan: A closed-loop ml-based planning benchmark for
557 autonomous vehicles. *arXiv preprint arXiv:2106.11810*, 2021.
- 558
559 CARLA Team, Intel Autonomous Agents Lab, the Embodied AI Foundation, and AlphaDrive. The
560 carla autonomous driving leaderboard. <https://leaderboard.carla.org/>, 2023.
- 561 Long Chen, Yuchen Li, Chao Huang, Yang Xing, Daxin Tian, Li Li, Zhongxu Hu, Siyu Teng,
562 Chen Lv, Jinjun Wang, et al. Milestones in autonomous driving and intelligent vehicles—part i:
563 Control, computing system design, communication, hd map, testing, and human behaviors. *IEEE*
564 *Transactions on Systems, Man, and Cybernetics: Systems*, 53(9):5831–5847, 2023.
- 565 Daniel Dauner, Marcel Hallgarten, Tianyu Li, Xinshuo Weng, Zhiyu Huang, Zetong Yang,
566 Hongyang Li, Igor Gilitschenski, Boris Ivanovic, Marco Pavone, Andreas Geiger, and Kashyap
567 Chitta. Navsim: Data-driven non-reactive autonomous vehicle simulation and benchmarking.
568 *arXiv*, 2406.15349, 2024.
- 569
570 Prafulla Dhariwal and Alexander Nichol. Diffusion models beat gans on image synthesis. *Advances*
571 *in neural information processing systems*, 34:8780–8794, 2021.
- 572 Alexey Dosovitskiy, German Ros, Felipe Codevilla, Antonio Lopez, and Vladlen Koltun. Carla: An
573 open urban driving simulator. In *Conference on robot learning*, pp. 1–16. PMLR, 2017.
- 574
575 Daocheng Fu, Wenjie Lei, Licheng Wen, Pinlong Cai, Song Mao, Min Dou, Botian Shi, and Yu Qiao.
576 Limsim++: A closed-loop platform for deploying multimodal llms in autonomous driving. *arXiv*
577 *preprint arXiv:2402.01246*, 2024a.
- 578 Daocheng Fu, Xin Li, Licheng Wen, Min Dou, Pinlong Cai, Botian Shi, and Yu Qiao. Drive like
579 a human: Rethinking autonomous driving with large language models. In *Proceedings of the*
580 *IEEE/CVF Winter Conference on Applications of Computer Vision*, pp. 910–919, 2024b.
- 581
582 Ruiyuan Gao, Kai Chen, Enze Xie, Lanqing Hong, Zhenguo Li, Dit-Yan Yeung, and Qiang
583 Xu. Magicdrive: Street view generation with diverse 3d geometry control. *arXiv preprint*
584 *arXiv:2310.02601*, 2023.
- 585 Shenyuan Gao, Jiazhi Yang, Li Chen, Kashyap Chitta, Yihang Qiu, Andreas Geiger, Jun Zhang,
586 and Hongyang Li. Vista: A generalizable driving world model with high fidelity and versatile
587 controllability. *arXiv preprint arXiv:2405.17398*, 2024.
- 588
589 Cole Gulino, Justin Fu, Wenjie Luo, George Tucker, Eli Bronstein, Yiren Lu, Jean Harb, Xinlei Pan,
590 Yan Wang, Xiangyu Chen, et al. Waymax: An accelerated, data-driven simulator for large-scale
591 autonomous driving research. *Advances in Neural Information Processing Systems*, 36, 2024.
- 592
593 Yuwei Guo, Ceyuan Yang, Anyi Rao, Yaohui Wang, Yu Qiao, Dahua Lin, and Bo Dai. Animatediff:
Animate your personalized text-to-image diffusion models without specific tuning. *arXiv preprint*
arXiv:2307.04725, 2023a.

- 594 Zhiming Guo, Xing Gao, Jianlan Zhou, Xinyu Cai, and Botian Shi. Scenedm: Scene-level multi-
595 agent trajectory generation with consistent diffusion models. *arXiv preprint arXiv:2311.15736*,
596 2023b.
- 597 Mordechai Haklay and Patrick Weber. Openstreetmap: User-generated street maps. *IEEE Pervasive*
598 *computing*, 7(4):12–18, 2008.
- 600 Yingqing He, Tianyu Yang, Yong Zhang, Ying Shan, and Qifeng Chen. Latent video diffusion
601 models for high-fidelity long video generation. *arXiv preprint arXiv:2211.13221*, 2022.
- 602 Anthony Hu, Lloyd Russell, Hudson Yeo, Zak Murez, George Fedoseev, Alex Kendall, Jamie Shot-
603 ton, and Gianluca Corrado. Gaia-1: A generative world model for autonomous driving. *arXiv*
604 *preprint arXiv:2309.17080*, 2023a.
- 606 Shengchao Hu, Li Chen, Penghao Wu, Hongyang Li, Junchi Yan, and Dacheng Tao. St-p3: End-to-
607 end vision-based autonomous driving via spatial-temporal feature learning. In *European Confer-*
608 *ence on Computer Vision*, pp. 533–549. Springer, 2022.
- 610 Yihan Hu, Jiazhi Yang, Li Chen, Keyu Li, Chonghao Sima, Xizhou Zhu, Siqi Chai, Senyao Du,
611 Tianwei Lin, Wenhai Wang, et al. Planning-oriented autonomous driving. In *Proceedings of the*
612 *IEEE/CVF Conference on Computer Vision and Pattern Recognition*, pp. 17853–17862, 2023b.
- 613 Xiaosong Jia, Zhenjie Yang, Qifeng Li, Zhiyuan Zhang, and Junchi Yan. Bench2drive: To-
614 wards multi-ability benchmarking of closed-loop end-to-end autonomous driving. *arXiv preprint*
615 *arXiv:2406.03877*, 2024.
- 616 Bo Jiang, Shaoyu Chen, Qing Xu, Bencheng Liao, Jiajie Chen, Helong Zhou, Qian Zhang, Wenyu
617 Liu, Chang Huang, and Xinggang Wang. Vad: Vectorized scene representation for efficient au-
618 tonomous driving. In *Proceedings of the IEEE/CVF International Conference on Computer Vi-*
619 *sion*, pp. 8340–8350, 2023.
- 621 Daniel Krajzewicz, Jakob Erdmann, Michael Behrisch, and Laura Bieker. Recent development and
622 applications of sumo-simulation of urban mobility. *International journal on advances in systems*
623 *and measurements*, 5(3&4), 2012.
- 624 Pengxiang Li, Zhili Liu, Kai Chen, Lanqing Hong, Yunzhi Zhuge, Dit-Yan Yeung, Huchuan Lu,
625 and Xu Jia. Trackdiffusion: Multi-object tracking data generation via diffusion models. *arXiv*
626 *preprint arXiv:2312.00651*, 2023a.
- 628 Quanyi Li, Zhenghao Peng, Lan Feng, Qihang Zhang, Zhenghai Xue, and Bolei Zhou. Metadrive:
629 Composing diverse driving scenarios for generalizable reinforcement learning. *IEEE transactions*
630 *on pattern analysis and machine intelligence*, 45(3):3461–3475, 2022a.
- 631 Xiaofan Li, Yifu Zhang, and Xiaoqing Ye. Drivingdiffusion: Layout-guided multi-view driving
632 scene video generation with latent diffusion model. *arXiv preprint arXiv:2310.07771*, 2023b.
- 634 Xin Li, Botian Shi, Yuenan Hou, Xingjiao Wu, Tianlong Ma, Yikang Li, and Liang He. Homoge-
635 neous multi-modal feature fusion and interaction for 3d object detection. In *European Conference*
636 *on Computer Vision*, pp. 691–707. Springer, 2022b.
- 637 Xin Li, Yeqi Bai, Pinlong Cai, Licheng Wen, Daocheng Fu, Bo Zhang, Xuemeng Yang, Xinyu
638 Cai, Tao Ma, Jianfei Guo, et al. Towards knowledge-driven autonomous driving. *arXiv preprint*
639 *arXiv:2312.04316*, 2023c.
- 641 Xin Li, Tao Ma, Yuenan Hou, Botian Shi, Yuchen Yang, Youquan Liu, Xingjiao Wu, Qin Chen,
642 Yikang Li, Yu Qiao, et al. Logonet: Towards accurate 3d object detection with local-to-global
643 cross-modal fusion. In *Proceedings of the IEEE/CVF Conference on Computer Vision and Pattern*
644 *Recognition*, pp. 17524–17534, 2023d.
- 645 Yuheng Li, Haotian Liu, Qingyang Wu, Fangzhou Mu, Jianwei Yang, Jianfeng Gao, Chunyuan Li,
646 and Yong Jae Lee. Gligen: Open-set grounded text-to-image generation. In *Proceedings of the*
647 *IEEE/CVF Conference on Computer Vision and Pattern Recognition*, pp. 22511–22521, 2023e.

- 648 Zhiqi Li, Zhiding Yu, Shiyi Lan, Jiahan Li, Jan Kautz, Tong Lu, and Jose M Alvarez. Is ego status
649 all you need for open-loop end-to-end autonomous driving? In *Proceedings of the IEEE/CVF*
650 *Conference on Computer Vision and Pattern Recognition*, pp. 14864–14873, 2024.
- 651
- 652 Cheng Lu, Yuhao Zhou, Fan Bao, Jianfei Chen, Chongxuan Li, and Jun Zhu. Dpm-solver: A fast
653 ode solver for diffusion probabilistic model sampling in around 10 steps. *Advances in Neural*
654 *Information Processing Systems*, 35:5775–5787, 2022.
- 655
- 656 Tao Ma, Xuemeng Yang, Hongbin Zhou, Xin Li, Botian Shi, Junjie Liu, Yuchen Yang, Zhizheng
657 Liu, Liang He, Yu Qiao, et al. Detzero: Rethinking offboard 3d object detection with long-term
658 sequential point clouds. In *Proceedings of the IEEE/CVF International Conference on Computer*
659 *Vision*, pp. 6736–6747, 2023.
- 660 Jianbiao Mei, Yu Yang, Mengmeng Wang, Tianxin Huang, Xuemeng Yang, and Yong Liu. Ssc-rs:
661 Elevate lidar semantic scene completion with representation separation and bev fusion. In *2023*
662 *IEEE/RSJ International Conference on Intelligent Robots and Systems (IROS)*, pp. 1–8. IEEE,
663 2023a.
- 664 Jianbiao Mei, Yu Yang, Mengmeng Wang, Zizhang Li, Xiaojun Hou, Jongwon Ra, Lajjian Li, and
665 Yong Liu. Centerlps: Segment instances by centers for lidar panoptic segmentation. In *Proceed-*
666 *ings of the 31st ACM International Conference on Multimedia*, pp. 1884–1894, 2023b.
- 667
- 668 Jianbiao Mei, Yu Yang, Mengmeng Wang, Junyu Zhu, Xiangrui Zhao, Jongwon Ra, Lajjian Li, and
669 Yong Liu. Camera-based 3d semantic scene completion with sparse guidance network. *arXiv*
670 *preprint arXiv:2312.05752*, 2023c.
- 671
- 672 Jianbiao Mei, Yukai Ma, Xuemeng Yang, Licheng Wen, Xinyu Cai, Xin Li, Daocheng Fu, Bo Zhang,
673 Pinlong Cai, Min Dou, et al. Continuously learning, adapting, and improving: A dual-process
674 approach to autonomous driving. *arXiv preprint arXiv:2405.15324*, 2024a.
- 675
- 676 Jianbiao Mei, Yu Yang, Mengmeng Wang, Zizhang Li, Jongwon Ra, and Yong Liu. Lidar video
677 object segmentation with dynamic kernel refinement. *Pattern Recognition Letters*, 178:21–27,
678 2024b.
- 679
- 680 Chenlin Meng, Yutong He, Yang Song, Jiaming Song, Jiajun Wu, Jun-Yan Zhu, and Stefano Ermon.
681 Sdedit: Guided image synthesis and editing with stochastic differential equations. *arXiv preprint*
arXiv:2108.01073, 2021.
- 682
- 683 Ben Mildenhall, Pratul P Srinivasan, Matthew Tancik, Jonathan T Barron, Ravi Ramamoorthi, and
684 Ren Ng. Nerf: Representing scenes as neural radiance fields for view synthesis. *Communications*
685 *of the ACM*, 65(1):99–106, 2021.
- 686
- 687 Chong Mou, Xintao Wang, Liangbin Xie, Yanze Wu, Jian Zhang, Zhongang Qi, and Ying Shan.
688 T2i-adapter: Learning adapters to dig out more controllable ability for text-to-image diffusion
689 models. In *Proceedings of the AAAI Conference on Artificial Intelligence*, volume 38, pp. 4296–
4304, 2024.
- 690
- 691 Alex Nichol, Prafulla Dhariwal, Aditya Ramesh, Pranav Shyam, Pamela Mishkin, Bob McGrew,
692 Ilya Sutskever, and Mark Chen. Glide: Towards photorealistic image generation and editing with
693 text-guided diffusion models. *arXiv preprint arXiv:2112.10741*, 2021.
- 694
- 695 William Peebles and Saining Xie. Scalable diffusion models with transformers. In *Proceedings of*
the IEEE/CVF International Conference on Computer Vision, pp. 4195–4205, 2023.
- 696
- 697 Dustin Podell, Zion English, Kyle Lacey, Andreas Blattmann, Tim Dockhorn, Jonas Müller, Joe
698 Penna, and Robin Rombach. Sdxl: Improving latent diffusion models for high-resolution image
699 synthesis. *arXiv preprint arXiv:2307.01952*, 2023.
- 700
- 701 Can Qin, Shu Zhang, Ning Yu, Yihao Feng, Xinyi Yang, Yingbo Zhou, Huan Wang, Juan Car-
los Niebles, Caiming Xiong, Silvio Savarese, et al. Unicontrol: A unified diffusion model for
controllable visual generation in the wild. *arXiv preprint arXiv:2305.11147*, 2023.

- 702 Alec Radford, Jong Wook Kim, Chris Hallacy, Aditya Ramesh, Gabriel Goh, Sandhini Agarwal,
703 Girish Sastry, Amanda Askell, Pamela Mishkin, Jack Clark, et al. Learning transferable visual
704 models from natural language supervision. In *International conference on machine learning*, pp.
705 8748–8763. PMLR, 2021.
- 706 Aditya Ramesh, Prafulla Dhariwal, Alex Nichol, Casey Chu, and Mark Chen. Hierarchical text-
707 conditional image generation with clip latents. *arXiv preprint arXiv:2204.06125*, 1(2):3, 2022.
- 708
709 Stephan R Richter, Vibhav Vineet, Stefan Roth, and Vladlen Koltun. Playing for data: Ground truth
710 from computer games. In *Computer Vision—ECCV 2016: 14th European Conference, Amsterdam,*
711 *The Netherlands, October 11–14, 2016, Proceedings, Part II 14*, pp. 102–118. Springer, 2016.
- 712
713 Darren Robinson, Frédéric Haldi, Philippe Leroux, Diane Perez, Adil Rasheed, and Urs Wilke.
714 Citysim: Comprehensive micro-simulation of resource flows for sustainable urban planning. In
715 *Proceedings of the Eleventh International IBPSA Conference*, pp. 1083–1090, 2009.
- 716
717 Robin Rombach, Andreas Blattmann, Dominik Lorenz, Patrick Esser, and Björn Ommer. High-
718 resolution image synthesis with latent diffusion models. In *Proceedings of the IEEE/CVF confer-*
719 *ence on computer vision and pattern recognition*, pp. 10684–10695, 2022.
- 720
721 German Ros, Laura Sellart, Joanna Materzynska, David Vazquez, and Antonio M Lopez. The
722 synthia dataset: A large collection of synthetic images for semantic segmentation of urban scenes.
723 In *Proceedings of the IEEE conference on computer vision and pattern recognition*, pp. 3234–
724 3243, 2016.
- 725
726 Chonghao Sima, Katrin Renz, Kashyap Chitta, Li Chen, Hanxue Zhang, Chengen Xie, Ping Luo,
727 Andreas Geiger, and Hongyang Li. Drivelm: Driving with graph visual question answering. *arXiv*
preprint arXiv:2312.14150, 2023.
- 728
729 Pei Sun, Henrik Kretschmar, Xerxes Dotiwalla, Aurelien Chouard, Vijaysai Patnaik, Paul Tsui,
730 James Guo, Yin Zhou, Yuning Chai, Benjamin Caine, et al. Scalability in perception for au-
731 tonomous driving: Waymo open dataset. In *Proceedings of the IEEE/CVF conference on com-*
732 *puter vision and pattern recognition*, pp. 2446–2454, 2020.
- 733
734 Tao Sun, Mattia Segu, Janis Postels, Yuxuan Wang, Luc Van Gool, Bernt Schiele, Federico Tombari,
735 and Fisher Yu. Shift: a synthetic driving dataset for continuous multi-task domain adaptation.
736 In *Proceedings of the IEEE/CVF Conference on Computer Vision and Pattern Recognition*, pp.
737 21371–21382, 2022.
- 738
739 Alexander Swerdlow, Runsheng Xu, and Bolei Zhou. Street-view image generation from a bird’s-
740 eye view layout. *IEEE Robotics and Automation Letters*, 2024.
- 741
742 U.S. Department of Transportation Federal Highway Administration. Next Generation Simulation
743 (NGSIM) Vehicle Trajectories and Supporting Data. Dataset, 2016. URL [http://doi.org/](http://doi.org/10.21949/1504477)
744 [10.21949/1504477](http://doi.org/10.21949/1504477). Accessed YYYY-MM-DD.
- 745
746 Wenhai Wang, Jiangwei Xie, ChuanYang Hu, Haoming Zou, Jianan Fan, Wenwen Tong, Yang Wen,
747 Silei Wu, Hanming Deng, Zhiqi Li, et al. Drivelm: Aligning multi-modal large language models
748 with behavioral planning states for autonomous driving. *arXiv preprint arXiv:2312.09245*, 2023a.
- 749
750 Xiaofeng Wang, Zheng Zhu, Guan Huang, Xinze Chen, and Jiwen Lu. Drivedreamer: Towards real-
751 world-driven world models for autonomous driving. *arXiv preprint arXiv:2309.09777*, 2023b.
- 752
753 Xiaofeng Wang, Zheng Zhu, Yunpeng Zhang, Guan Huang, Yun Ye, Wenbo Xu, Ziwei Chen, and
754 Xingang Wang. Are we ready for vision-centric driving streaming perception? the asap bench-
755 mark. In *Proceedings of the IEEE/CVF Conference on Computer Vision and Pattern Recognition*,
pp. 9600–9610, 2023c.
- 756
757 Yan Wang, Yi Liu, Shijie Zhao, Junlin Li, and Li Zhang. Camixers: Only details need more” atten-
758 tion”. In *Proceedings of the IEEE/CVF Conference on Computer Vision and Pattern Recognition*,
pp. 25837–25846, 2024.

- 756 Licheng Wen, Pinlong Cai, Daocheng Fu, Song Mao, and Yikang Li. Bringing diversity to au-
757 tonomous vehicles: An interpretable multi-vehicle decision-making and planning framework.
758 In *Proceedings of the 2023 International Conference on Autonomous Agents and Multiagent*
759 *Systems, AAMAS '23*, pp. 2571–2573, Richland, SC, 2023a. International Foundation for Au-
760 tonomous Agents and Multiagent Systems. ISBN 9781450394321.
- 761 Licheng Wen, Daocheng Fu, Xin Li, Xinyu Cai, Tao Ma, Pinlong Cai, Min Dou, Botian Shi, Liang
762 He, and Yu Qiao. Dilu: A knowledge-driven approach to autonomous driving with large language
763 models. *arXiv preprint arXiv:2309.16292*, 2023b.
- 764 Licheng Wen, Daocheng Fu, Song Mao, Pinlong Cai, Min Dou, Yikang Li, and Yu Qiao. Lim-
765 sim: A long-term interactive multi-scenario traffic simulator. In *2023 IEEE 26th International*
766 *Conference on Intelligent Transportation Systems (ITSC)*, pp. 1255–1262. IEEE, 2023c.
- 768 Yuqing Wen, Yucheng Zhao, Yingfei Liu, Fan Jia, Yanhui Wang, Chong Luo, Chi Zhang, Tiancai
769 Wang, Xiaoyan Sun, and Xiangyu Zhang. Panacea: Panoramic and controllable video generation
770 for autonomous driving. In *Proceedings of the IEEE/CVF Conference on Computer Vision and*
771 *Pattern Recognition*, pp. 6902–6912, 2024.
- 772 Wei Wu, Xiaoxin Feng, Ziyang Gao, and Yuheng Kan. Smart: Scalable multi-agent real-time simu-
773 lation via next-token prediction. *arXiv preprint arXiv:2405.15677*, 2024.
- 774 Zirui Wu, Tianyu Liu, Liyi Luo, Zhide Zhong, Jianteng Chen, Hongmin Xiao, Chao Hou, Haozhe
775 Lou, Yuantao Chen, Runyi Yang, et al. Mars: An instance-aware, modular and realistic simulator
776 for autonomous driving. In *CAAI International Conference on Artificial Intelligence*, pp. 3–15.
777 Springer, 2023.
- 779 Yang Xing, Chen Lv, Dongpu Cao, and Peng Hang. Toward human-vehicle collaboration: Review
780 and perspectives on human-centered collaborative automated driving. *Transportation research*
781 *part C: emerging technologies*, 128:103199, 2021.
- 782 Guohang Yan, Jiahao Pi, Jianfei Guo, Zhaotong Luo, Min Dou, Nianchen Deng, Qiusheng Huang,
783 Daocheng Fu, Licheng Wen, Pinlong Cai, et al. Oasim: an open and adaptive simulator based on
784 neural rendering for autonomous driving. *arXiv preprint arXiv:2402.03830*, 2024.
- 786 Jiazhi Yang, Shenyan Gao, Yihang Qiu, Li Chen, Tianyu Li, Bo Dai, Kashyap Chitta, Penghao Wu,
787 Jia Zeng, Ping Luo, et al. Generalized predictive model for autonomous driving. In *Proceedings*
788 *of the IEEE/CVF Conference on Computer Vision and Pattern Recognition*, pp. 14662–14672,
789 2024.
- 790 Kairui Yang, Enhui Ma, Jibin Peng, Qing Guo, Di Lin, and Kaicheng Yu. Bevcontrol: Accurately
791 controlling street-view elements with multi-perspective consistency via bev sketch layout. *arXiv*
792 *preprint arXiv:2308.01661*, 2023a.
- 793 Xuemeng Yang, Hao Zou, Xin Kong, Tianxin Huang, Yong Liu, Wanlong Li, Feng Wen, and
794 Hongbo Zhang. Semantic segmentation-assisted scene completion for lidar point clouds. In *2021*
795 *IEEE/RSJ International Conference on Intelligent Robots and Systems (IROS)*, pp. 3555–3562.
796 IEEE, 2021.
- 797 Ze Yang, Yun Chen, Jingkan Wang, Sivabalan Manivasagam, Wei-Chiu Ma, Anqi Joyce Yang, and
798 Raquel Urtasun. Unisim: A neural closed-loop sensor simulator. In *Proceedings of the IEEE/CVF*
799 *Conference on Computer Vision and Pattern Recognition*, pp. 1389–1399, 2023b.
- 800 Tengju Ye, Wei Jing, Chunyong Hu, Shikun Huang, Lingping Gao, Fangzhen Li, Jingke Wang,
801 Ke Guo, Wencong Xiao, Weibo Mao, et al. Fusionad: Multi-modality fusion for prediction and
802 planning tasks of autonomous driving. *arXiv preprint arXiv:2308.01006*, 2023.
- 803 Tianwei Yin, Xingyi Zhou, and Philipp Krahenbuhl. Center-based 3d object detection and tracking.
804 In *Proceedings of the IEEE/CVF conference on computer vision and pattern recognition*, pp.
805 11784–11793, 2021.
- 806 Jiang-Tian Zhai, Ze Feng, Jinhao Du, Yongqiang Mao, Jiang-Jiang Liu, Zichang Tan, Yifu Zhang,
807 Xiaoqing Ye, and Jingdong Wang. Rethinking the open-loop evaluation of end-to-end autonomous
808 driving in nuscenec. *arXiv preprint arXiv:2305.10430*, 2023.
- 809

810 Lvmin Zhang, Anyi Rao, and Maneesh Agrawala. Adding conditional control to text-to-image
811 diffusion models. In *Proceedings of the IEEE/CVF International Conference on Computer Vision*,
812 pp. 3836–3847, 2023.

813
814 Jianbo Zhao, Jiaheng Zhuang, Qibin Zhou, Taiyu Ban, Ziyao Xu, Hangning Zhou, Junhe Wang,
815 Guoan Wang, Zhiheng Li, and Bin Li. Kigras: Kinematic-driven generative model for realistic
816 agent simulation. *arXiv preprint arXiv:2407.12940*, 2024a.

817 Shihao Zhao, Dongdong Chen, Yen-Chun Chen, Jianmin Bao, Shaozhe Hao, Lu Yuan, and Kwan-
818 Yee K Wong. Uni-controlnet: All-in-one control to text-to-image diffusion models. *Advances in*
819 *Neural Information Processing Systems*, 36, 2024b.

820
821 Yunsong Zhou, Michael Simon, Zhenghao Peng, Sicheng Mo, Hongzi Zhu, Minyi Guo, and
822 Bolei Zhou. Simgen: Simulator-conditioned driving scene generation. *arXiv preprint*
823 *arXiv:2406.09386*, 2024.

824
825
826
827
828
829
830
831
832
833
834
835
836
837
838
839
840
841
842
843
844
845
846
847
848
849
850
851
852
853
854
855
856
857
858
859
860
861
862
863

A APPENDIX

CONTENTS

864
865
866
867
868
869
870
871
872
873
874
875
876
877
878
879
880
881
882
883
884
885
886
887
888
889
890
891
892
893
894
895
896
897
898
899
900
901
902
903
904
905
906
907
908
909
910
911
912
913
914
915
916
917

A.1 Related Works 17

 A.1.1 Data Acquisition for Autonomous driving 17

 A.1.2 Diffusion-based Generative Models 18

 A.1.3 Evolution of Autonomous Driving Generation 18

 A.1.4 Simulator-Driven Scenario Generation 18

 A.1.5 Closed-Loop Driving in Simulation 19

A.2 Implementation Details 19

 A.2.1 World Dreamer Setups 19

 A.2.2 Traffic Manager Setups 19

A.3 Visualization of World Dreamer 20

A.4 Visualization of open-loop and close-loop experiments 24

A.5 Corner Case Generation through IntSIM 29

A.6 Future Work 30

A.1 RELATED WORKS

Table 4: Comparison of various datasets, generative models, world models, and simulators in terms of interactivity, fidelity, and diversity features. **DATA.** represents dataset, **GEN.** represents generative model, **W.M.** represents world model, **SIM.** represents simulator.

Type	Name	Interactivity		Fidelity			Diversity		
		Uncontrollable Closed-loop	Controllable Closed-loop	Realistic Images	Real-world Roadgraph	daylight/weather	Different Images	Multi-view Video	Unlimited Unspecified map
DATA.	CitySim (Robinson et al., 2009) / NGSIM	X	X	X	✓	X	X	X	X
	Bench2Drive (Jia et al., 2024)	X	X	X	X	✓	✓	X	X
	DriveLM-CARLA (Sima et al., 2023)	X	X	X	X	✓	✓	X	X
	nuPlan dataset (Caesar et al., 2021)	X	X	✓	✓	X	✓	X	X
	nuScenes (Caesar et al., 2020) / Waymo dataset (Sun et al., 2020)	X	X	✓	✓	X	✓	X	X
GEN.	MagicDrive (Gao et al., 2023) / DriveDreamer (Wang et al., 2023b)	X	X	✓	✓	✓	✓	X	X
	SimGen (Zhou et al., 2024)	X	X	✓	✓	✓	✓	X	X
W.M.	KiGRAS (Zhao et al., 2024a) / SMART (Wu et al., 2024)	✓	X	X	✓	X	X	X	✓
	MUVO (Bogdoll et al., 2023)	✓	X	X	✓	X	X	X	X
	Vista (Gao et al., 2024) / GAIA-1 (Hu et al., 2023a)	✓	X	X	X	✓	X	X	X
SIM.	Waymax (Gulino et al., 2024)	✓	✓	X	✓	X	X	X	X
	SUMO (Krajzewicz et al., 2012) / LimSim (Wen et al., 2023c)	✓	✓	X	✓	X	X	X	✓
	CARLA (Dosovitskiy et al., 2017)	✓	✓	X	✓	X	✓	✓	✓
	MetaDrive (Li et al., 2022a)	✓	✓	✓	✓	X	✓	✓	✓
	Unisim (Yang et al., 2023b) / OAsim (Yan et al., 2024)	✓	✓	✓	✓	X	✓	X	X
Ours	DRIVEARENA	✓	✓	✓	✓	✓	✓	✓	✓

A.1.1 DATA ACQUISITION FOR AUTONOMOUS DRIVING

The characteristics of the automated driving dataset can be categorized into two aspects: appearance fidelity and interactivity. First, regarding appearance fidelity, NGSIM (U.S. Department of Transportation Federal Highway Administration, 2016) and CitySim (Robinson et al., 2009) provide only realistic driving trajectories that can provide safe and reliable driving planning guidance. On top of that, some datasets developed based on the Carla simulator, such as DriveLM-CARLA (Sima et al., 2023) and Bench2Drive (Jia et al., 2024), provide simulated sensor data. Taking it a step further, the Waymo (Sun et al., 2020) and nuScenes (Caesar et al., 2020) datasets capture real-world sensor recordings and the driving behavior of human drivers. The datasets were produced in a complex process and with limited data. To add variety to the scenarios, MagicDrive (Gao et al., 2023) and DriveDreamer (Wang et al., 2023b) provide editable scenario generation. So far, we have obtained diverse and rich data for training. However, the above data can only be used for open-loop evaluation, i.e., current decisions do not affect future data distributions, which differs significantly from

918 actual driving. Works (Hu et al., 2023a; Gao et al., 2024; Bogdoll et al., 2023; Zhao et al., 2024a;
919 Wu et al., 2024) that also have fidelity differences improve the interactivity of the data, they usually
920 use auto-regressive generation methods to realize the interaction, the generation process implies the
921 model’s understanding of the world. Usually, it can not be too much human intervention. Some
922 simulators (Gulino et al., 2024; Wen et al., 2023c; Li et al., 2022a; Dosovitskiy et al., 2017; Yang
923 et al., 2023b; Yan et al., 2024; Krajzewicz et al., 2012) make things more controllable by decoupling
924 part of the mechanics of how the world works. Common examples include simulators (Krajzewicz
925 et al., 2012; Gulino et al., 2024; Wen et al., 2023c) that provide realistic traffic flow, and simula-
926 tors (Dosovitskiy et al., 2017; Li et al., 2022a) that drive vehicles in game engines, and reconstruc-
927 tive simulations represented by (Yang et al., 2023b; Yan et al., 2024) that provide the appearance of
928 reality.

929 930 A.1.2 DIFFUSION-BASED GENERATIVE MODELS

931
932 Recent advancements in generative models have seen diffusion models play a pivotal role in image
933 and video generation (Dhariwal & Nichol, 2021; Meng et al., 2021; Nichol et al., 2021; Podell et al.,
934 2023; Ramesh et al., 2022; Blattmann et al., 2023; He et al., 2022). Moreover, recent works have
935 expanded the scope by integrating additional control signals beyond traditional text prompts (Guo
936 et al., 2023a; Li et al., 2023e; Mou et al., 2024). For instance, ControlNet (Zhang et al., 2023)
937 incorporates a trainable version of the SD encoder for control signals, while studies such as Uni-
938 ControlNet (Zhao et al., 2024b) and UniControl (Qin et al., 2023) have emphasized the fusion of
939 multi-modal inputs into a unified control condition using input-level adapter structures. Our ap-
940 proach aims to study the generation of continuous and controllable sequence frames, thereby bridg-
941 ing the gap between simulation environments and reality, and establishing the required foundation
942 for closed-loop learning of autonomous driving agents.

943 944 A.1.3 EVOLUTION OF AUTONOMOUS DRIVING GENERATION

945
946 World Models (Hu et al., 2023a; Yang et al., 2024) utilize diffusion models to generate future driving
947 scenes based on historical information. These methods often lack the ability to control the scenarios
948 through layout, are difficult to generate continuous and stable videos and lack the approximation of
949 physical laws.

950 TrackDiffusion focused on generating videos based on 2D object layouts (Li et al., 2023a). BEV-
951 Gen (Swerdlow et al., 2024) pioneered the generation of synthetic multi-view images based on the
952 BEV layout, laying the foundation for a controllable generation of autonomous driving scenarios.
953 BEVControl (Yang et al., 2023a) extended this approach by a height elevation process, enabling im-
954 age generation aligned with surrounding projection layouts. Further advancements includes Mag-
955 icDrive (Gao et al., 2023), DriveDreamer (Wang et al., 2023b), Panacea (Wen et al., 2024) and
956 DrivingDiffusion (Li et al., 2023b), which generate panoramic controllable videos through various
957 3D controls and encoding strategies. However, their primary focus lies in augmenting training data
958 to enhance algorithm performance, rather than serving as simulators for modeling dynamic environ-
959 mental interactions.

960 961 A.1.4 SIMULATOR-DRIVEN SCENARIO GENERATION

962
963 Autonomous vehicle development is significantly enhanced by driving simulators, which provide
964 controlled environments for realistic simulation. Prominent research efforts have concentrated on
965 generating virtual imagery and annotations, with some studies expanding to incorporate environ-
966 mental variations and construct safety-critical scenarios for training based on real-world data logs.
967 Nevertheless, these simulated images frequently fall short of achieving true realism, as evidenced
968 by previous works (Ros et al., 2016; Richter et al., 2016; Sun et al., 2022). While SimGen (Zhou
969 et al., 2024) made a breakthrough as the first work to generate diverse driving scenarios following
970 conditions from a simulated environment, it mainly focused on the quality of the generated content
971 with only front-view images, neglecting the exploration of closed-loop systems. Our research aims
to bridge this gap by developing a system that can not only generate realistic scenarios but also allow
agents to interact with them in a closed-loop manner.

972 A.1.5 CLOSED-LOOP DRIVING IN SIMULATION

973
974 End-to-end vehicle control algorithms (Hu et al., 2022; 2023b; Ye et al., 2023), are typically trained
975 and evaluated on open-loop datasets (Caesar et al., 2020). However, these algorithms lack the capa-
976 bility to generalize directly to simulators for closed-loop evaluation, which hinders the demonstra-
977 tion of their true performance potential. Recent studies have increasingly recognized the significance
978 of closed-loop evaluation, as exemplified by (Jiang et al., 2023; Wang et al., 2023a). Moreover, sim-
979 ulation environments offer a wealth of training data, a stark contrast to models trained on datasets
980 that are constrained by data distribution (Li et al., 2024). A significant challenge arises due to the
981 discrepancy between the simulated scene’s appearance and real-world conditions, complicating the
982 generalization of models trained on simulation data to actual scenarios. This creates a paradox: the
983 desire to utilize simulation data for its diversity and editability, while also seeking data that closely
984 mirrors reality. Our approach effectively addresses this issue by enhancing the realism of the simu-
985 lator for certain closed-loop learning methods (Mei et al., 2024a).

986 A.2 IMPLEMENTATION DETAILS

987 A.2.1 WORLD DREAMER SETUPS

988 **Dataset.** For World Dreamer, we use the nuScenes (Caesar et al., 2020) dataset for training. Fol-
989 lowing the official configuration, we employ 700 scenes for training and 150 for validation. We
990 focus on four road categories (lane boundary, lane divider, pedestrian crossing, and drivable area)
991 and ten object categories. The nuScenes dataset contains data collected from four different cities,
992 covering various light and weather conditions, including daytime, night, sunny, cloudy, and rainy
993 scenarios, enabling DRIVEARENA to conditionally imitate diverse appearances. We additionally an-
994 notated each scene using GPT-4V, providing detailed scene descriptions that include elements like
995 time, weather, street style, road structure, and appearance. These descriptions serve as text prompt
996 conditions.
997

998 **Model Setup.** The model is initialized with the pre-trained Stable Diffusion v1.5 (Rombach et al.,
999 2022), with only the newly added parameters being trained. For various conditions, except for the
1000 encoding of reference images and text prompts, the encoders for other conditions are randomly
1001 initialized and trained from scratch. These conditions are then integrated into the UNet using a
1002 randomly initialized ControlNet (Zhang et al., 2023) to control the denoising process.
1003

1004 **Training and Inference.** To utilize the reference images and achieve temporal correlation, we
1005 employ ASAP (Wang et al., 2023c) to generate 12Hz interpolated annotations and crop them into
1006 image clips of length $n = 7$. During training, we use the last frame of each clip as the current frame,
1007 select any frame from the clip as the reference frame, and calculate the relative pose between them to
1008 model the motion trend of the background. Accordingly, the surround images corresponding to the
1009 reference frame are input to the network as reference images. During inference, the generated result
1010 of the previous frame is used as the current reference images, enabling unlimited length generation.
1011 The experiment is conducted on 8 NVIDIA A100 (80GB) GPUs with a batch size of 4×8 and 200K
1012 iterations of training. The AdamW optimizer is used with a learning rate of $1e-4$. The network
1013 follows the same image resolution (224×400) as MagicDrive, and when input to the driving agent,
1014 it will be upsampled to the original image size of nuScenes (900×1600) through a super-resolution
1015 algorithm (Wang et al., 2024).

1016 A.2.2 TRAFFIC MANAGER SETUPS

1017 **Operating Frequencies.** In our experiments, the Traffic Manager operates at a frequency of 10Hz,
1018 while the control frequency is set to 2Hz. This configuration results in the Traffic Manager sending
1019 the current layout to World Dreamer every 0.5 simulation seconds, requesting surround images.
1020 These images are then forwarded to the driving agent, which predicts and plans the subsequent
1021 trajectory for the ego vehicle. The Traffic Manager, World Dreamer, and driving agent communicate
1022 via HTTP protocol, enabling deployment across different servers.
1023

1024 **Simulation Modes.** As detailed in Section 3.4, we implement two simulation modes. In the open-
1025 loop mode, all vehicles, including the ego vehicle, are controlled by Traffic Manager itself. The
driving agent can predict the ego vehicle’s trajectory, but its trajectory is not actually executed. In the

1026 closed-loop mode, the ego vehicle is controlled by the driving agent, and the simulation terminates
1027 if it crashes with other vehicles or leaves the road.

1028 **Supported Maps.** Currently, DRIVEARENA supports four different maps, which
1029 are: `singapore-onenorth`, `boston-seaport`, `boston-thomaspark`, and
1030 `carla-town05`. The first two maps closely resemble the corresponding areas in the nuScenes
1031 dataset, while the last one replicates the road network of the Town05 map in the CARLA simulator.
1032 Notably, Traffic Manager can download road network data for any area directly from Open-
1033 StreetMap and perform simulations, enabling DRIVEARENA to simulate the road network of almost
1034 any city worldwide. Our map processing pipeline employs a two-stage approach using SUMO
1035 tools to enhance OSM’s road-level information. First, we utilize OSMWebWizard to download
1036 OSM maps and establish topological roadnet. Second, we employ the `randomTrips` script to
1037 generate vehicle demands and their corresponding origin-destination pairs within the map. Beyond
1038 these pre-simulation processes, we support several customization options where users can modify
1039 downloaded OSM maps, create custom maps manually, or convert OpenDRIVE format maps to our
1040 supported format.

1041 A.3 VISUALIZATION OF WORLD DREAMER

1042 In this section, we will comprehensively demonstrate the controllability and scalability of the model
1043 from various dimensions, including the control of lighting and weather, the fit of object boxes and
1044 maps, change of street style, and consistency over long periods of time.

1045 We conducted an experiment by setting up two identical traffic scenes sharing the same road network
1046 and traffic participants, varying only the ego vehicle’s position. The results generated by World
1047 Dreamer, shown in Figure 8, demonstrate how the model handles scene consistency when the ego
1048 vehicle moves from the leftmost to the middle lane. World Dreamer successfully maintains spatial
1049 consistency in lane markings and surrounding vehicle positions while preserving similar street styles
1050 and building configurations. However, due to the inherent stochastic nature of diffusion models,
1051 minor variations emerge in vehicle colors and street backgrounds.

1052 We demonstrate the impact of the reference image on the generated image, as shown in Figure 7.
1053 We randomly select one frame of images from the nuScenes dataset as reference images and choose
1054 three scenes from OpenStreetMap and Carla. We perform inference on them with World Dreamer
1055 respectively. It can be seen that the source and style of the road network are very different from
1056 the scope of the original nuScenes dataset. The pictures show that the generated vehicles and road
1057 networks conform closely to control conditions, demonstrating strong control capabilities. The style
1058 and weather of the generated pictures can also be consistent with the reference images. In other
1059 words, besides maintaining image generation continuity through reference images, we can also reg-
1060 ulate image style accordingly.

1061 In addition to the two weather generation examples shown in Figure 5, Figure 9 presents two more
1062 demonstrations, further highlighting the controllability and fidelity of World Dreamer. These four
1063 sets of images display notable variations in weather and lighting while consistently maintaining their
1064 distinct styles throughout the continuous iteration process.

1065 We demonstrate additional cases using data from the nuPlan dataset to validate the scalability. The
1066 nuPlan data originates from cities different from nuScenes and features varying camera numbers and
1067 parameters. We select 6 cameras with a similar layout to the nuScenes dataset, and nuPlan’s camera
1068 parameters are employed to project object boxes and lane lines onto corresponding images as control
1069 conditions. As shown in Figure 10, World Dreamer which only trained on nuScenes adeptly adheres
1070 to these conditions, generating coherent images when deployed in new cities and even with novel
1071 camera configurations.

1072 In addition, we trained a version of World Dreamer using a mixed training dataset combining both
1073 nuPlan and nuScenes datasets. While maintaining the same model architecture, we found that World
1074 Dreamer can generate street view images in the distinctive styles of Las Vegas and Pittsburgh, which
1075 are exclusively present in the nuPlan dataset. The results are shown in Figure 11, where we can
1076 observe the characteristic Las Vegas Strip with its palm trees, as well as the distinctive low-rise
1077 buildings of Pittsburgh. By incorporating more diverse driving data, we successfully enhanced the
1078 generative model’s capability to generalize across different urban environments.

1079

1080
1081
1082
1083
1084
1085
1086
1087
1088
1089
1090
1091
1092
1093
1094
1095
1096
1097
1098
1099
1100
1101
1102
1103
1104
1105
1106
1107
1108
1109
1110
1111
1112
1113
1114
1115
1116
1117
1118
1119
1120
1121
1122
1123
1124
1125
1126
1127
1128
1129
1130
1131
1132
1133

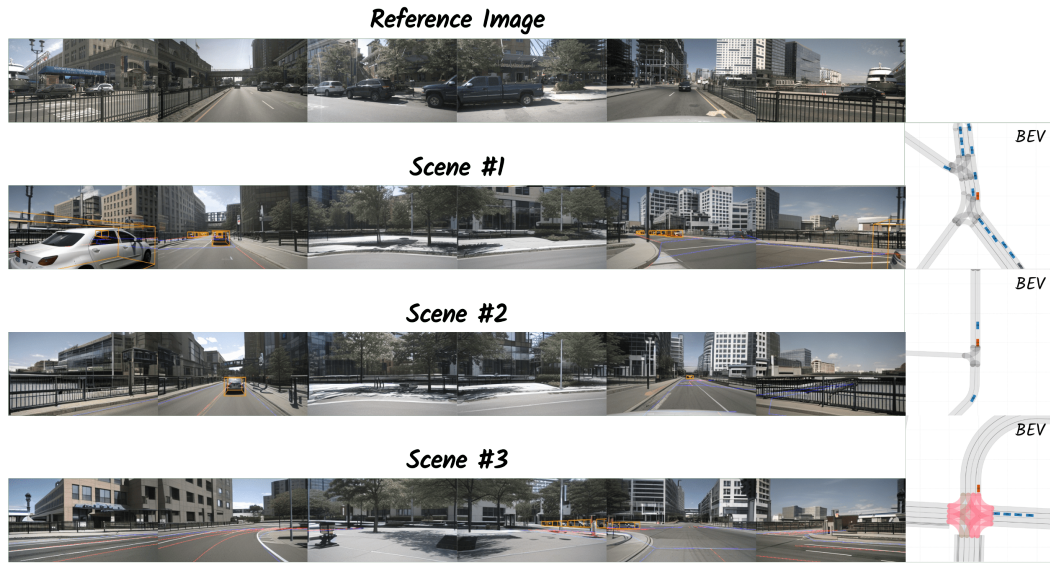


Figure 7: Demonstration of reference image influence on generated scenes. Three scenes are presented, all derived from a single nuScenes reference frame. Despite notable variations in road networks, World Dreamer successfully integrates street styles and weather conditions from the reference image while adhering to specified control conditions for vehicles and road layouts. Of particular interest is the aerial corridor visible in the reference image, which is accurately reproduced in scenes #1 and #2. However, in scene #3, due to the curved road configuration, the corridor is not generated, illustrating World Dreamer’s adaptability to different road geometries.

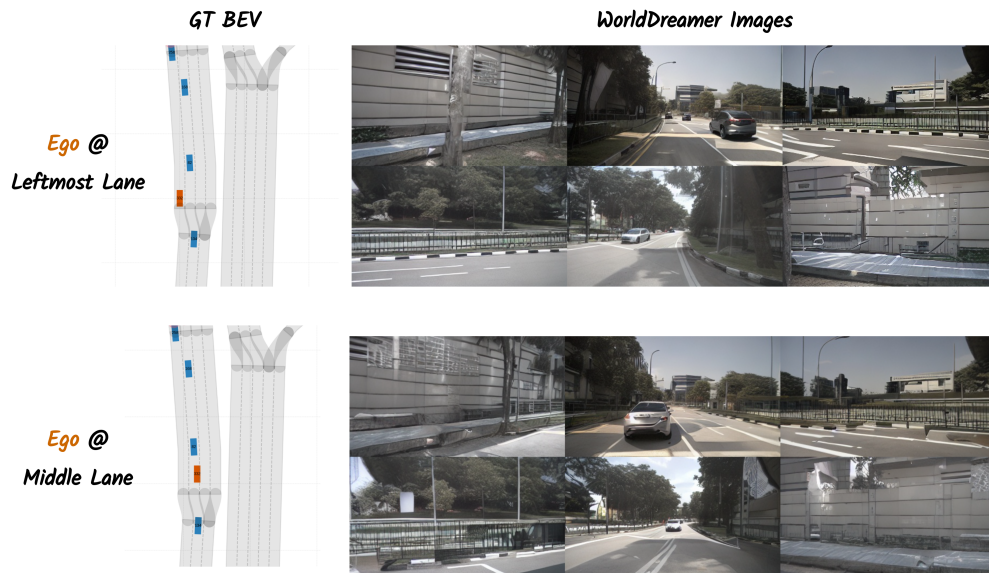
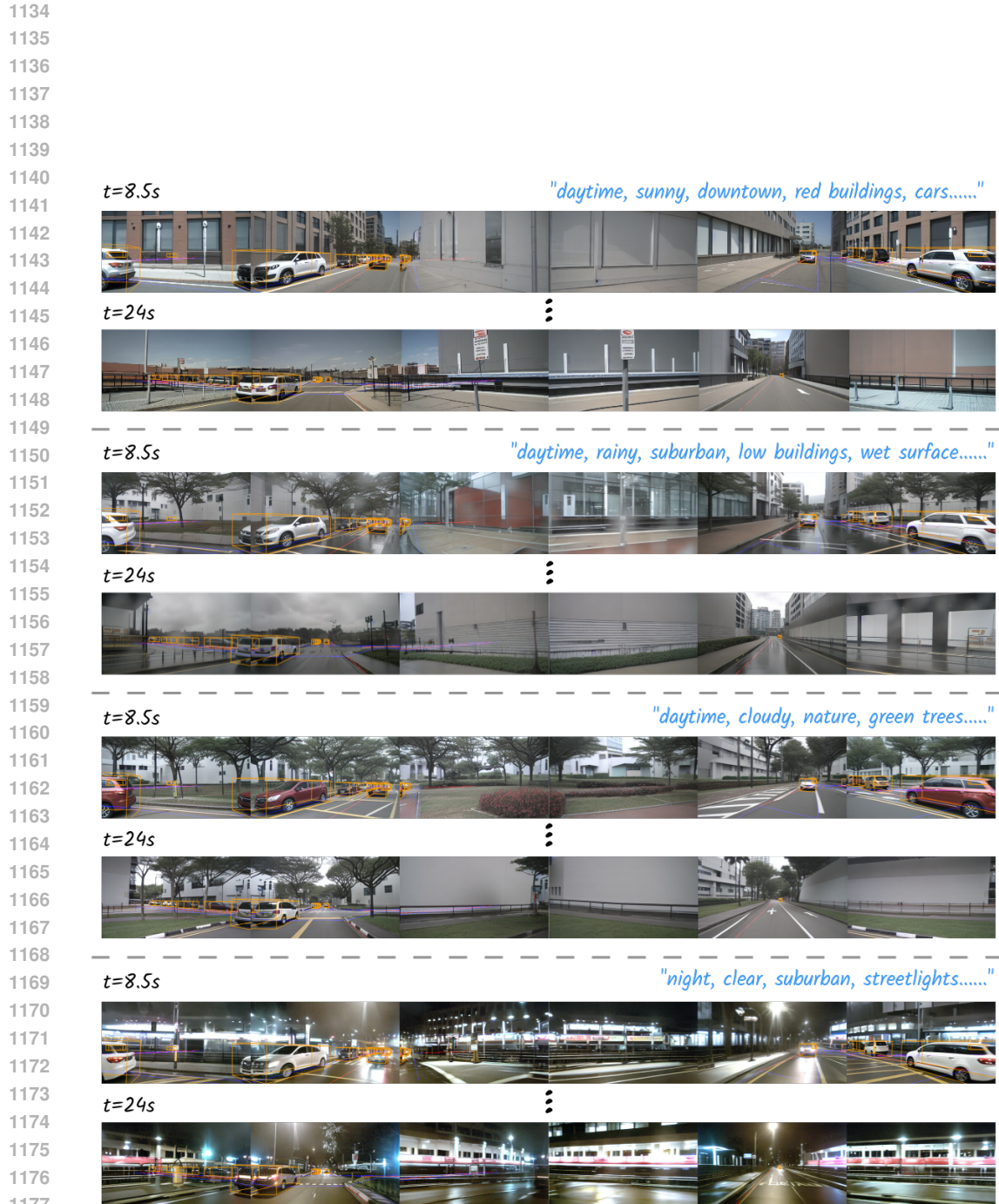


Figure 8: Demonstration of generated images from identical traffic scenarios with varying ego positions. The two scenes share the same road network and traffic participants, with the ego vehicle position shifting from the leftmost to the middle lane. While minor variations appear in front vehicle color and street backgrounds, World Dreamer maintains consistent lane markings and spatial relationships of surrounding vehicles, preserving similar street styles and building configurations.



1179 Figure 9: Demonstration of diverse prompts and reference images' influence on identical scenes.
1180 The figure presents four distinct image sequences generated by DRIVEARENA for the same 30-
1181 second simulation sequence, each utilizing different prompts and reference images. All sequences
1182 strictly adhere to the provided control conditions for road structures and vehicles, maintaining cross-
1183 view consistency. Notably, the four sequences exhibit significant variations in weather and lighting
1184 conditions while consistently preserving their respective styles throughout the entire 30-second du-
1185 ration.

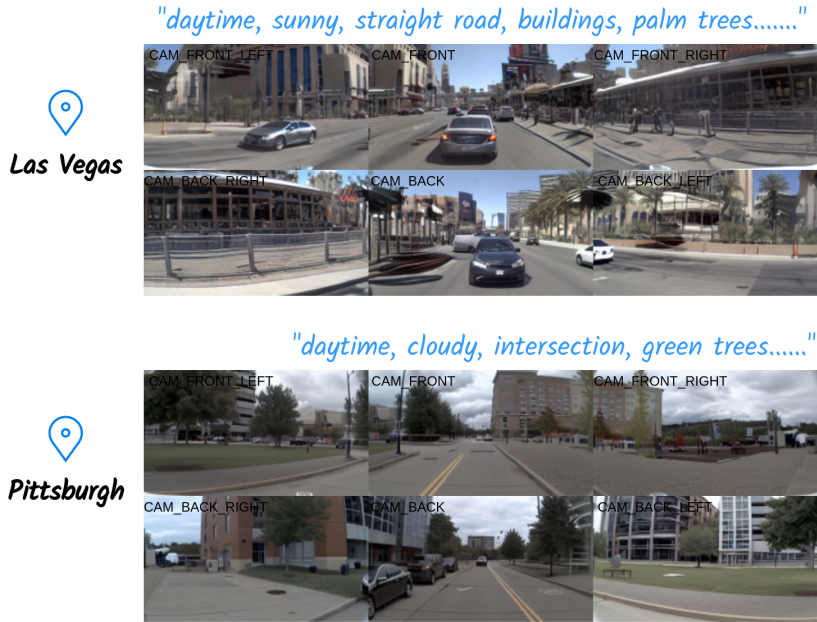
1186
1187

1188
1189
1190
1191
1192
1193
1194
1195
1196
1197
1198
1199
1200
1201
1202
1203
1204
1205
1206



1207
1208 Figure 10: Zero-shot inference on nuPlan datasets. World Dreamer, trained exclusively on the
1209 nuScenes dataset, demonstrates remarkable adaptability when applied to the nuPlan dataset. The
1210 latter comprises data from new cities (Pittsburgh, Las Vegas) that are not present in nuScenes, with
1211 different camera configurations and parameters. We selected three nuPlan scenes and directly utilized
1212 nuPlan’s camera parameters to project object boxes and lane lines onto the corresponding
1213 images as control conditions. The results show that World Dreamer produces coherent images when
1214 deployed in unfamiliar cities and even with previously unseen camera configurations and layouts.

1215
1216
1217
1218
1219
1220
1221
1222
1223
1224
1225
1226
1227
1228
1229
1230
1231
1232
1233
1234
1235
1236



1237 Figure 11: World Dreamer inference on nuPlan locations. Using a mixed training dataset from both
1238 nuPlan and nuScenes, World Dreamer demonstrates the ability to generate street view images capturing
1239 the distinctive styles of Las Vegas and Pittsburgh—locations exclusive to the nuPlan dataset. This
1240 enhanced training approach with diverse driving data significantly improves World Dreamer’s
1241 generalization capability.

1242 A.4 VISUALIZATION OF OPEN-LOOP AND CLOSE-LOOP EXPERIMENTS 1243

1244 In DRIVEARENA’s open-loop mode, Figure 12 and Figure 13 illustrate two additional sequences
1245 on top of Figure 6, demonstrating that the prediction from the driving agents on the road network
1246 and vehicle tracking is fundamentally accurate. However, in terms of metrics, performance from
1247 both agents in such scenarios with unseen road and traffic flow is significantly degraded, with an
1248 average PDM Score of only 0.636 for UniAD and an average PDM Score of 0.683 for VAD. The
1249 output trajectories exhibit a substantial increase in collision rates and instances of driving outside
1250 the drivable area.

1251 Figure 14 illustrates two failure cases where UniAD lacked sufficient trajectory correction capabil-
1252 ities. Despite a roughly correct prediction of the road structure, it ultimately mounted the central
1253 green belt or failed to complete a right turn successfully. The average Arena Driving Score for
1254 UniAD is 0.086, while VAD achieves only 0.025 on average. Two failure cases resulting from the
1255 VAD’s closed-loop evaluation in DRIVEARENA are presented in Figure 15. In failure case 1, the
1256 driving agent ran onto the central tree lawn while recognizing the right road boundary compara-
1257 tively correctly. In Failure Case 2, the VAD incorrectly predicted the left-turn roadway structure as
1258 a straight roadway and, therefore, could not successfully complete the left turn. These cases demon-
1259 strate the importance of closed-loop evaluation in reflecting the true capabilities of AD agents, and
1260 also show that our DRIVEARENA demonstrates good ability in following the road structure.

1261 It should be noted that these are preliminary results based on testing only 4 routes. We plan to
1262 expand the number of routes for a more comprehensive evaluation and explore the combined effect
1263 of World Dreamer’s timing consistency and the driver agent’s performance on the final ADS.
1264
1265
1266
1267
1268
1269
1270
1271
1272
1273
1274
1275
1276
1277
1278
1279
1280
1281
1282
1283
1284
1285
1286
1287
1288
1289
1290
1291
1292
1293
1294
1295

1296
1297
1298
1299
1300
1301
1302
1303
1304
1305
1306
1307
1308
1309
1310
1311
1312
1313
1314
1315
1316
1317
1318
1319
1320
1321
1322
1323
1324
1325
1326
1327
1328
1329
1330
1331
1332
1333
1334
1335
1336
1337
1338
1339
1340
1341
1342
1343
1344
1345
1346
1347
1348
1349

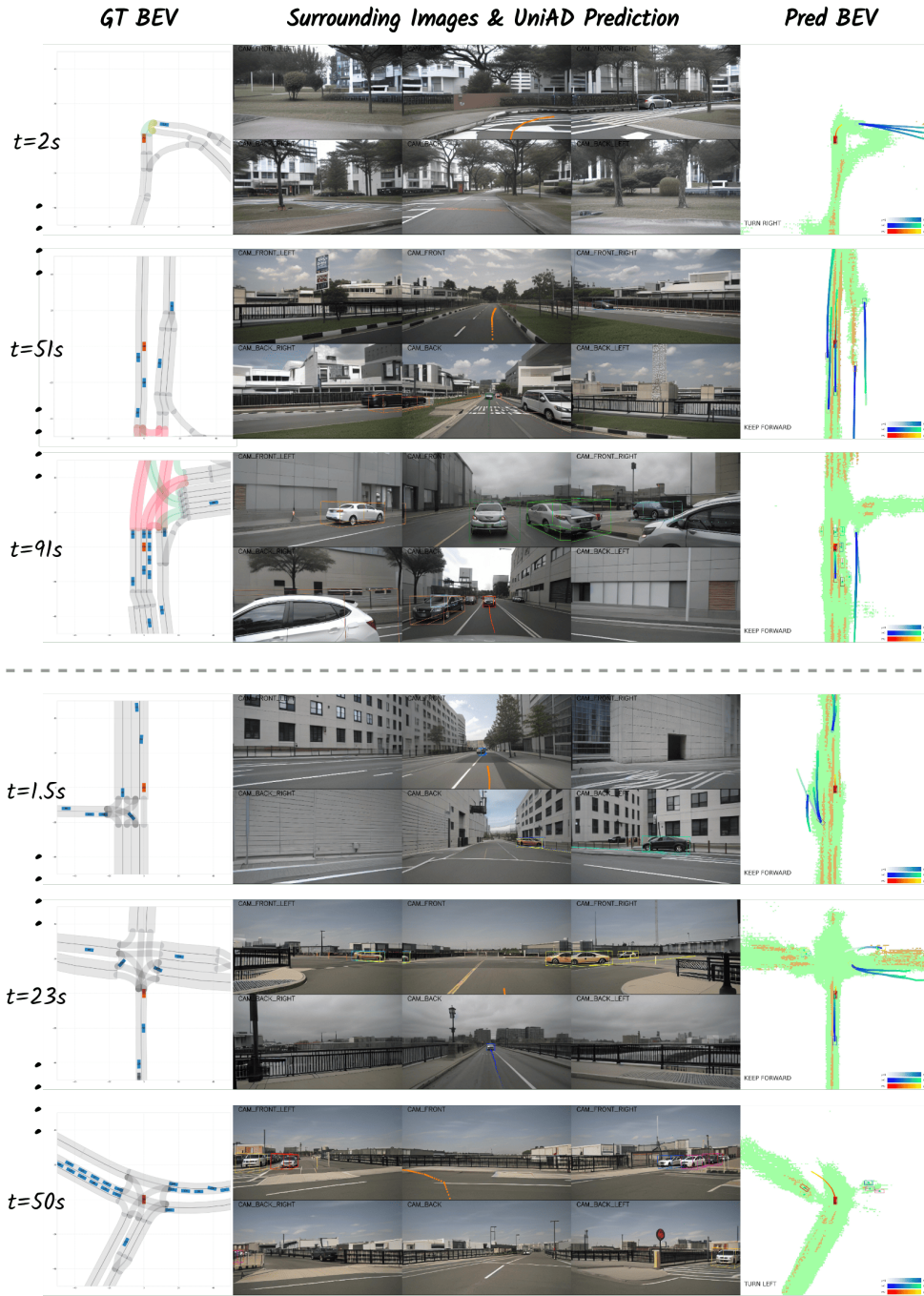


Figure 12: Case studies of UniAD’s open-loop performance in DRIVEARENA. The figure presents two long-term open-loop simulation sequences: the upper sequence depicts a Singapore road network and style (left-hand drive), while the lower sequence shows a Boston road network and style (right-hand drive). Each subfigure displays, from left to right: Traffic Manager’s ground truth BEV; World Dreamer-generated image with corresponding UniAD detection bounding boxes and predicted trajectories; and UniAD-predicted BEV image.

1350
 1351
 1352
 1353
 1354
 1355
 1356
 1357
 1358
 1359
 1360
 1361
 1362
 1363
 1364
 1365
 1366
 1367
 1368
 1369
 1370
 1371
 1372
 1373
 1374
 1375
 1376
 1377
 1378
 1379
 1380
 1381
 1382
 1383
 1384
 1385
 1386
 1387
 1388
 1389
 1390
 1391
 1392
 1393
 1394
 1395
 1396
 1397
 1398
 1399
 1400
 1401
 1402
 1403

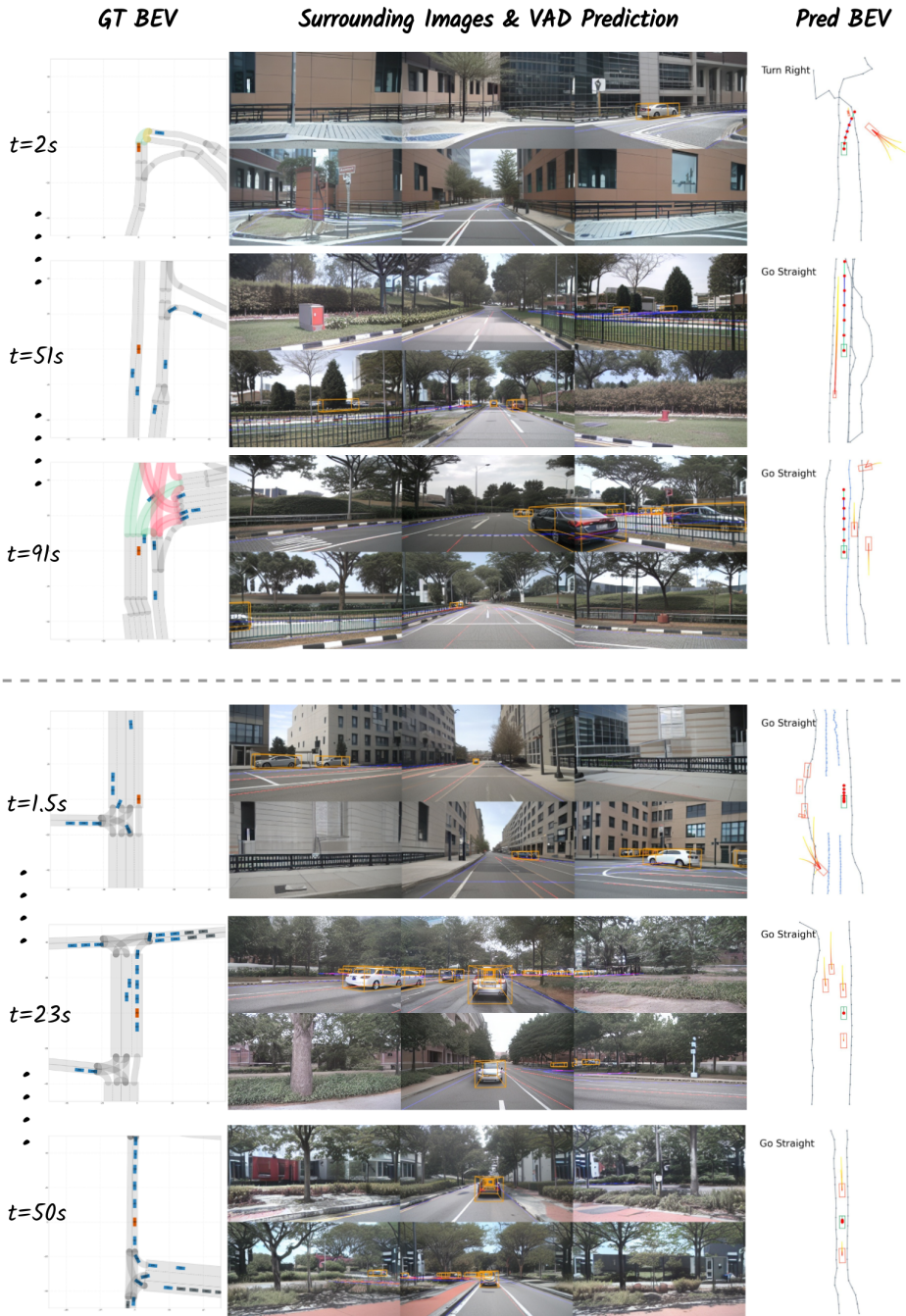


Figure 13: Examples of VAD’s open-loop performance in DRIVEARENA. The figure presents two long simulation sequences: the upper one captures a Singapore road network with left-hand driving, while the lower one shows a Boston road network with right-hand driving. Each subfigure provides, from left to right: the ground truth BEV from Traffic Manager; images generated by World Dreamer with ground truth layout; and VAD’s predicted BEV representation.

1404
 1405
 1406
 1407
 1408
 1409
 1410
 1411
 1412
 1413
 1414
 1415
 1416
 1417
 1418
 1419
 1420
 1421
 1422
 1423
 1424
 1425
 1426
 1427
 1428
 1429
 1430
 1431
 1432
 1433
 1434
 1435
 1436
 1437
 1438
 1439
 1440
 1441
 1442
 1443
 1444
 1445
 1446
 1447
 1448
 1449
 1450
 1451
 1452
 1453
 1454
 1455
 1456
 1457

Failure Case #1



Failure Case #2



Figure 14: Failure cases of UniAD in DRIVEARENA’s closed-loop mode. While UniAD generally predicts road structures accurately: (top) UniAD encroaching onto the central median; (bottom) UniAD failing to complete a right turn successfully.

1458
 1459
 1460
 1461
 1462
 1463
 1464
 1465
 1466
 1467
 1468
 1469
 1470
 1471
 1472
 1473
 1474
 1475
 1476
 1477
 1478
 1479
 1480
 1481
 1482
 1483
 1484
 1485
 1486
 1487
 1488
 1489
 1490
 1491
 1492
 1493
 1494
 1495
 1496
 1497
 1498
 1499
 1500
 1501
 1502
 1503
 1504
 1505
 1506
 1507
 1508
 1509
 1510
 1511

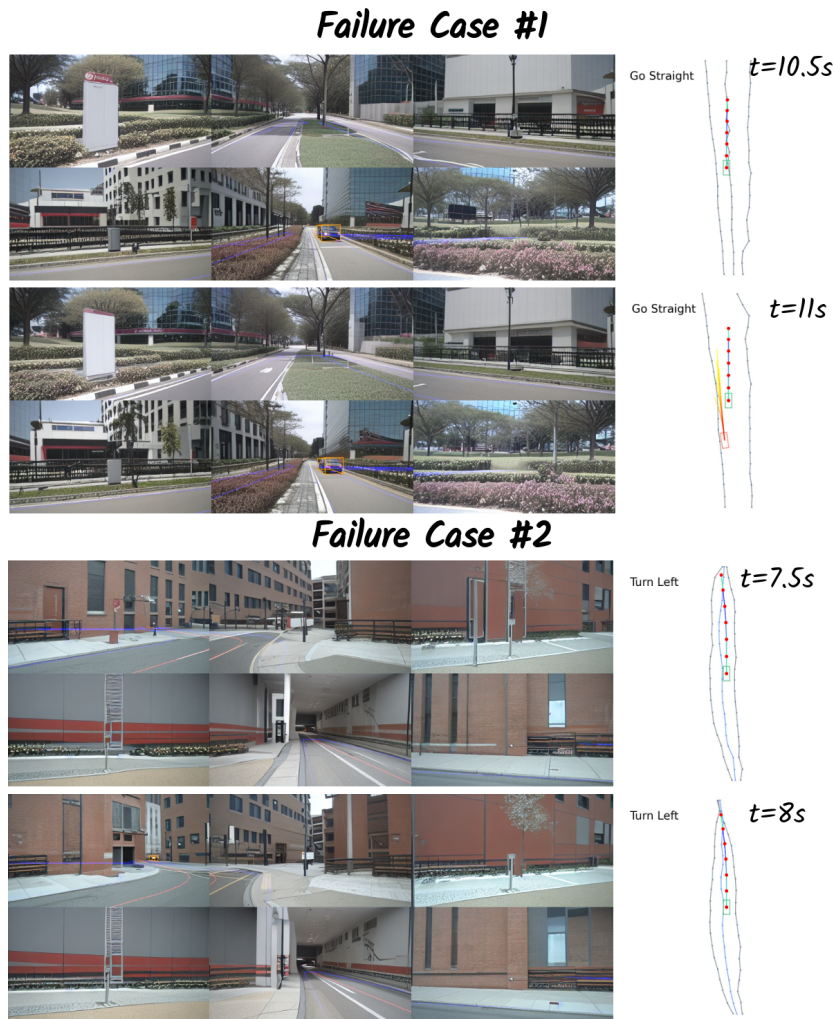


Figure 15: Examples of VAD failures in DRIVEARENA closed-loop mode. (Top) Although VAD was able to predict the road structure with basic accuracy, it drove onto the center greenbelt; (Bottom) VAD was unable to predict the left-turning road structure and therefore was unable to successfully complete the left turn.

A.5 CORNER CASE GENERATION THROUGH INTSIM

In this section, we demonstrate one application of DRIVEARENA: generating extreme case or accident scene replays. Specifically, we utilize an algorithm called IntSIM to simulate accident traffic flow, where an attacking vehicle intentionally collides with others. This simulation reveals rare and extreme scenarios, providing valuable insights for researchers and engineers to test and improve the safety features of driving agent algorithms. Furthermore, DRIVEARENA allows various perspectives to be adopted during the simulation, so that the ego vehicle can be the vehicle affected by the collision, the vehicle causing the collision, or an observer witnessing the event.

Figure 16 illustrates a collision simulation within DRIVEARENA, showing two scenarios in which traffic participants attack the ego vehicle. As shown in the figure, DRIVEARENA is able to effectively simulate these traffic flows and render realistic surround images. However, since World Dreamer is trained entirely on the nuScenes dataset, which lacks extreme and unsafe car accident event data, it is temporarily unable to simulate the post-crash state of the vehicle or the physical impact of the collision, which is also a direction worth exploring further.

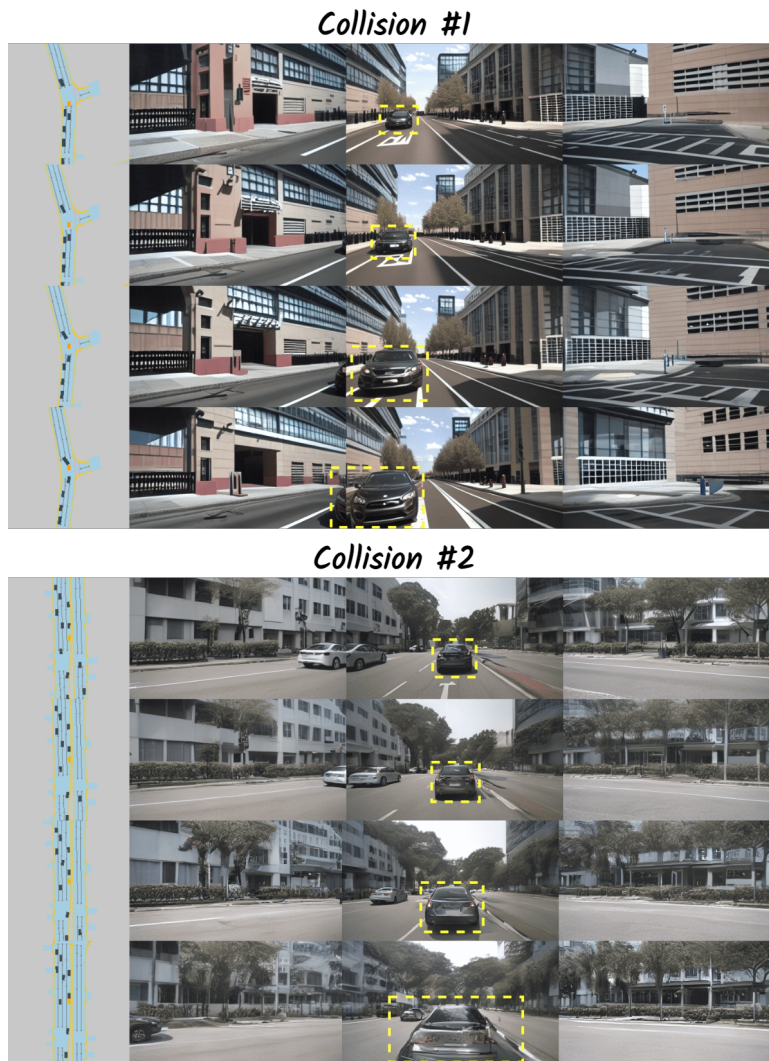


Figure 16: Simulated collision demonstrations within DRIVEARENA. Two extreme scenarios are shown in which one of the traffic participants initiates an attack on the ego vehicle while driving. The results show that the DRIVEARENA can handle these rare scenarios effectively. However, due to the limited availability of data on unsafe events, World Dreamer is unable to simulate the resulting vehicle damage or the physical impact of collisions.

1566 A.6 FUTURE WORK
1567

1568 In future work, the following limitations of the current DRIVEARENA implementation need to be
1569 addressed to improve its overall performance and capabilities:

1570 **1) Data Diversity:** The current generative model is trained solely on the nuScenes dataset, which
1571 limits the diversity and emergence capabilities. We plan to expand training to include more varied
1572 datasets to enhance the model’s robustness and versatility.

1573 **2) Temporal Consistency:** While we can generate continuous videos with an autoregression strat-
1574 egy, maintaining motion trends and temporal consistency between frames remains challenging. Fu-
1575 ture work will explore multi-frame autoregressive networks and more scalable architectures (Peebles
1576 & Xie, 2023) to address these issues.

1577 **3) Runtime Efficiency:** Like many generative models, World Dreamer requires significant runtime.
1578 Investigating faster sampling methods (Lu et al., 2022) and model quantization may alleviate these
1579 problems.

1580 **4) Expanded Agent Testing:** We plan to incorporate a broader range of driving agents within
1581 DRIVEARENA, facilitating the continuous learning and evolution of knowledge-driven driving
1582 agents in the closed-loop environment (Li et al., 2023c).

1583 **5) A Real Arena:** DRIVEARENA can not only evaluate the performance of different driving agents,
1584 but also act as a testing ground for AD generative models. Using the same driving agent as a referee
1585 can fairly assess the sim-to-real gap of different generative models. This approach even provides a
1586 more credible and convincing evaluation compared to traditional metrics like FID and FVD.

1587 We recognize that practical application may still be a way off, but the potential and promise shown
1588 by this work are evident. We hope this research will advance closed-loop exploration in highly
1589 realistic environments and offer a valuable platform for developing and assessing driving agents
1590 across a range of challenging scenarios. We encourage the community to collaborate in advancing
1591 this field. The era of open loops is transitioning, and autonomous driving evaluation and learning
1592 are set to enter a new era of closed-loop systems.

1593
1594
1595
1596
1597
1598
1599
1600
1601
1602
1603
1604
1605
1606
1607
1608
1609
1610
1611
1612
1613
1614
1615
1616
1617
1618
1619